CENOZOIC STRATIGRAPHY AND SLOPE PROCESSES, SOUTHWESTERN SCOTIAN SLOPE

Michael K. Giles

Submitted in Partial Fulfillment of the Requirements
For the Degree of Bachelor of Science, Honours

Department of Earth Sciences and Oceanography
Dalhousie University
Halifax, Nova Scotia
Canada

March 2007

DALHOUSIE UNIVERSITY
UNIVERSITY
Inspiring Minds

Department of Earth Sciences
Halifax, Nova Scotia
Canada B3H 4J1
(902) 494-2358
FAX (902) 494-6889

DATE: _____

AUTHOR: _____

TITLE: _____

_____

_____

_____

Degree: _____   Convocation: _____   Year: _____

Permission is herewith granted to Dalhousie University to circulate and to have copied for non-commercial purposes, at its discretion, the above title upon the request of individuals or institutions.

_____
Signature of Author

Abstract

Recent hydrocarbon exploration and scientific activity along on the southwestern Scotian Slope has provided the opportunity to improve the understanding of past and present sedimentation patterns and processes recorded on the slope. Eight seismic horizons in the Barrington 3D Cube were correlated in the dip and strike directions across the study area, creating the stratigraphic framework. The scope of this study is to explore the Cenozoic stratigraphy in terms of the mass transport complexes (MTC) and discern how these complexes have affected the evolution of the Scotian margin with particular emphasis within the Barrington Block (3D seismic cube provided by EnCana Corporation).

Four seismic facies (A, B, C, and D) were identified in the Barrington 3D seismic cube were used to distinguish and describe six units within the cube. Seismic facies interpretation of the cube demonstrates that the upper portion of the Scotian Slope was comprised of chaotic, discontinuous reflectors suggesting that the Cenozoic strata of the primarily records successive MTC deposits. Four of the six units observed in this study were identified as MTC deposits.

Four triggering mechanisms have been suggested to initiate MTC's along the Scotian margin: seismicity, glacial sediment overloading, gas hydrates and salt tectonics. Most likely the triggering events for these MTC's are some combination of the four mechanisms that cause instability along the Slope. The results and interpretation of these MTC deposits will help to improve the understanding of deep water basin development, slope evolution and assist in geo-hazard assessment of offshore Nova Scotia.

Key words: mass transport complexes (MTC), 3D seismic stratigraphy, seismic facies, Scotian Slope, Cenozoic stratigraphy, triggering mechanisms, slope processes, geo-hazards.

Table of Contents

Table of Figures

List of Tables

Acknowledgements

Chapter 1: Introduction

1.1 Introduction

Recent scientific and hydrocarbon exploration activity with modern survey technologies along the Scotian margin provides the opportunity to improve the understanding of sedimentation patterns and processes on the Scotian Slope. One of the major findings of these new data is the ubiquity of mass transport deposits. Improved understanding of the role of mass transport processes in margin development will lead to improved models of basin development and better assessment of modern geo-hazards that have the potential to improve deep water basin development offshore Nova Scotia.

1.2 Objectives

An exploration area on the southwestern Scotian Slope known as the Barrington block was chosen as a case study for this thesis. Seismic data within the area exhibit a history of mass failures, including deposits on the seafloor. This thesis will develop the Cenozoic stratigraphy, especially in terms of the mass transport deposits (MTD) and address how these events influenced the construction of the Scotian margin. These results will lead to improved models for deep water basin development and assist in geo-hazard assessments for potential offshore exploration and development.

The use of 3D seismic data provided by industry (EnCana) will greatly assist not only development of the Cenozoic stratigraphy and will allow detailed examination of the seismic geomorphology of MTD's to interpret processes of transportation, deposition and slope evolution.

1.3 Physiography

Throughout this thesis several terms will be used to describe the physiography of Novas Scotia's continental margin. The Atlantic margin consists of the continental shelf, slope and rise.

The continental shelf (Fig 1.1) is the flat portion of the margin with a slope angle less then 0.1° that extends from coastal land to a point offshore where the slope angle increases significantly, known as the shelf break (Thurman and Trujillo, 2002). Nova Scotia's continental shelf extends 150 to 200 km offshore and the shelf break lies at a depth of approximately 200 m (Piper and Sparkes, 1990).

The continental slope (Fig 1.1) begins at the shelf break and continues to the point where there is subtle change in gradient or locally to the abyssal plain (Emery and Uchupi, 1984). The angle of continental slope off Nova Scotia ranges between 1.5° to 4° (Campbell *et al.*, 2004) with an average of 3° (Thurman and Trujillo, 2002).

The continental rise (Fig 1.1) is the transition zone from the continental slope to the abyssal plain and is composed of sediment that has been eroded out of the continental slope (Thurman & Trujillo, 2002).
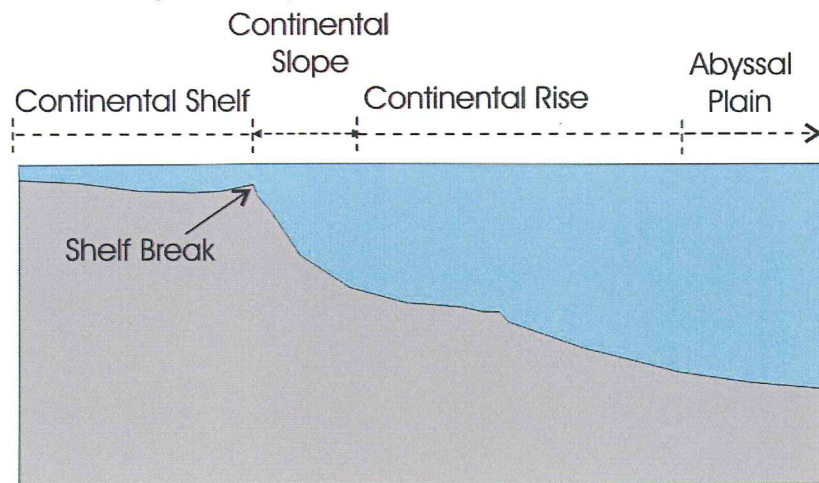
Figure 1.1 – A schematic of the components of the Atlantic Margin.

1.4 Study Area

The Scotian Slope is located along the western margin of the North Atlantic Ocean and extends for 1000 km from the Laurentian Channel in the east to the Northeast Channel in the west (Fig 1.2). It runs parallel to the Nova Scotia coastline in a east-west direction. The Scotian Slope is divided into an eastern, a central and a western section based on morphological features. The eastern portion of the Scotian Slope has a slope angle of between 2.5° to 4° and 500 m deep submarine canyons that dissect the slope and cut back into the continental shelf. The central portion has a shallower slope gradient of between 1.5° to 3° and does not have submarine canyons. The seabed is largely smooth with escarpments up to 80 m in height (Campbell *et al.*, 2004). The western portion appears as a re-entrant with a concave-up slope profile. There are no major canyons but there are channels transecting the slope and remnant ridges. The seafloor is rugged or rugose (Mosher *et al.*, 2004).

The study area (Fig 1.2) is located in the southwestern portion of the Scotian Slope (42°N to 43° N and 64° W to 65° W) in water depths from 750-2000 m.
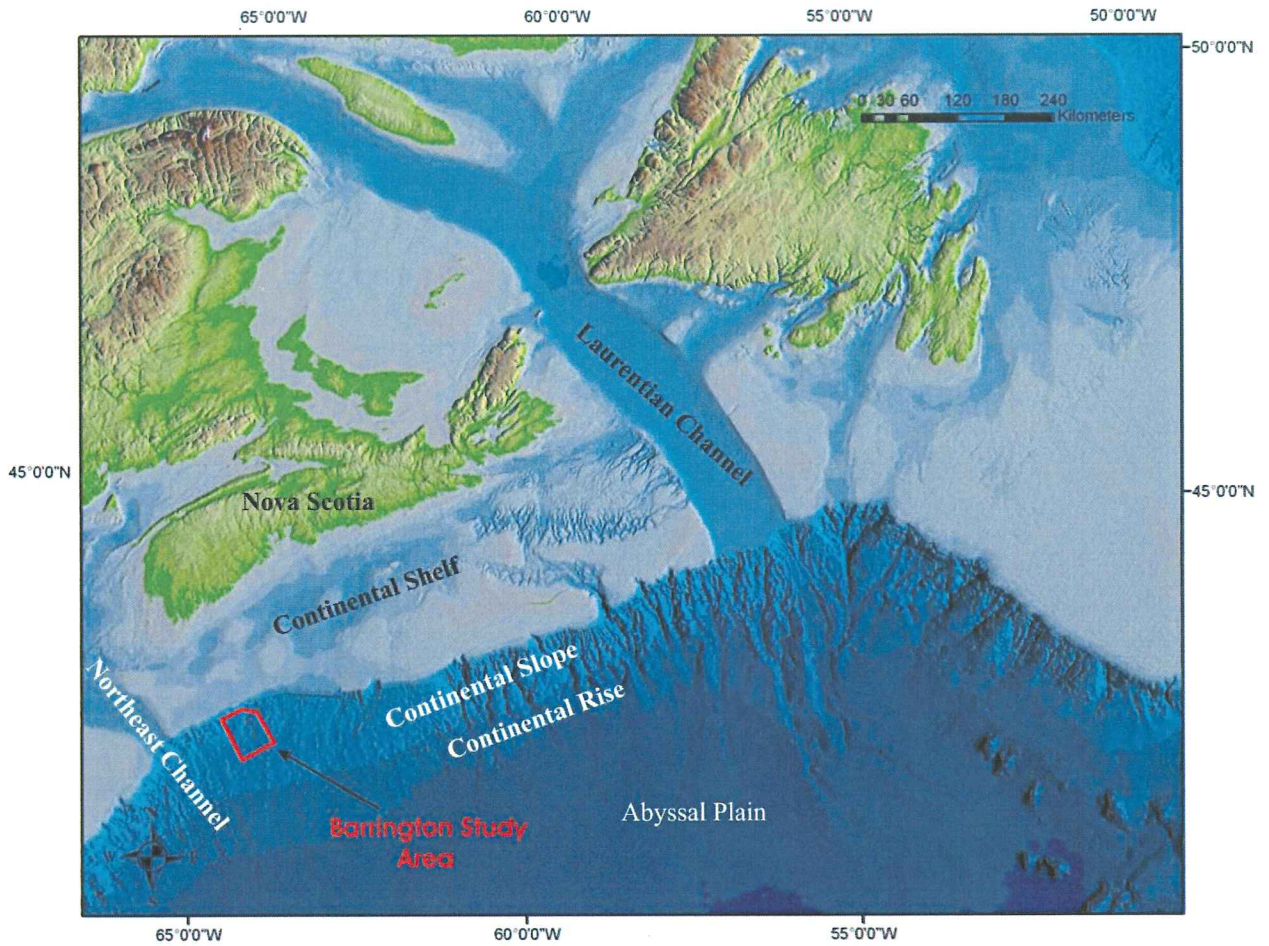
Figure 1.2 – Regional Map of the Scotian Slope with the Barrington study area is outlined in red. (Base map from Shaw and Courtney 2002).

Chapter 2: Geological Background

2.1 Tectonic Setting

A thorough synthesis of the tectonic development of the Scotian margin is provided by Wade and MacLean, (1990) and is summarized here. The Scotian margin is a passive continental margin formed during the Mesozoic Period. During the break up of Pangaea, the Scotian Basin was a lowland area on the northwestern side of the rift system, southwest from the Tethys Sea. Rifting began between the Late Permian and Late Triassic and led to the widening and lengthening of the Scotian Basin area until the early part of the Mesozoic. The Scotian Basin is infilled with Mesozoic-Cenozoic sediments on an accreted wedge, deposited on the flank of the Appalachian Orogen. It is flanked by the Yarmouth Arch to the southwest, the Avalon Uplift to the northeast and the LaHave Platform and Canso Ridge to the northwest (Fig 2.1). The Yarmouth Arch is a Mesozoic and Cenozoic element which forms the western limit for the major Triassic-Jurassic salt basin. The Avalon Uplift is a Late Jurassic component formed during seafloor spreading. It cut across the Jurassic Basins, uplifting it and increasing the amount of erosion with reworking of sediments during the Early Cretaceous. These sediments were deposited westward into the Scotian Basin (Wade and MacLean, 1990).

During development of the North Atlantic Ocean, a series of interconnected Mesozoic-Cenozoic depocenters formed off Nova Scotia as a result of horst and graben tectonics and salt tectonics. Sedimentation began in the Scotian Basin as early as the Middle Triassic possibly making it the earliest sediment deposition in Eastern Canadian basins except for the Jeanne D'Arc Basin. The sediments deposited in the Scotian Basin occurred in a northeast trending graben complex with redbeds at the base and

subsequence fill of redbeds and salt. Following this sequence was the deposition of a thick sequence of Jurassic sediments (Wade and MacLean, 1990).

The Scotian margin experienced three major periods of basement subsidence during the post-rifting events of the Jurassic, Cretaceous and Tertiary. These periods of basement subsidence resulted in the formation of the sedimentary sub-basins of the Scotian Basin (Louden, 2002).
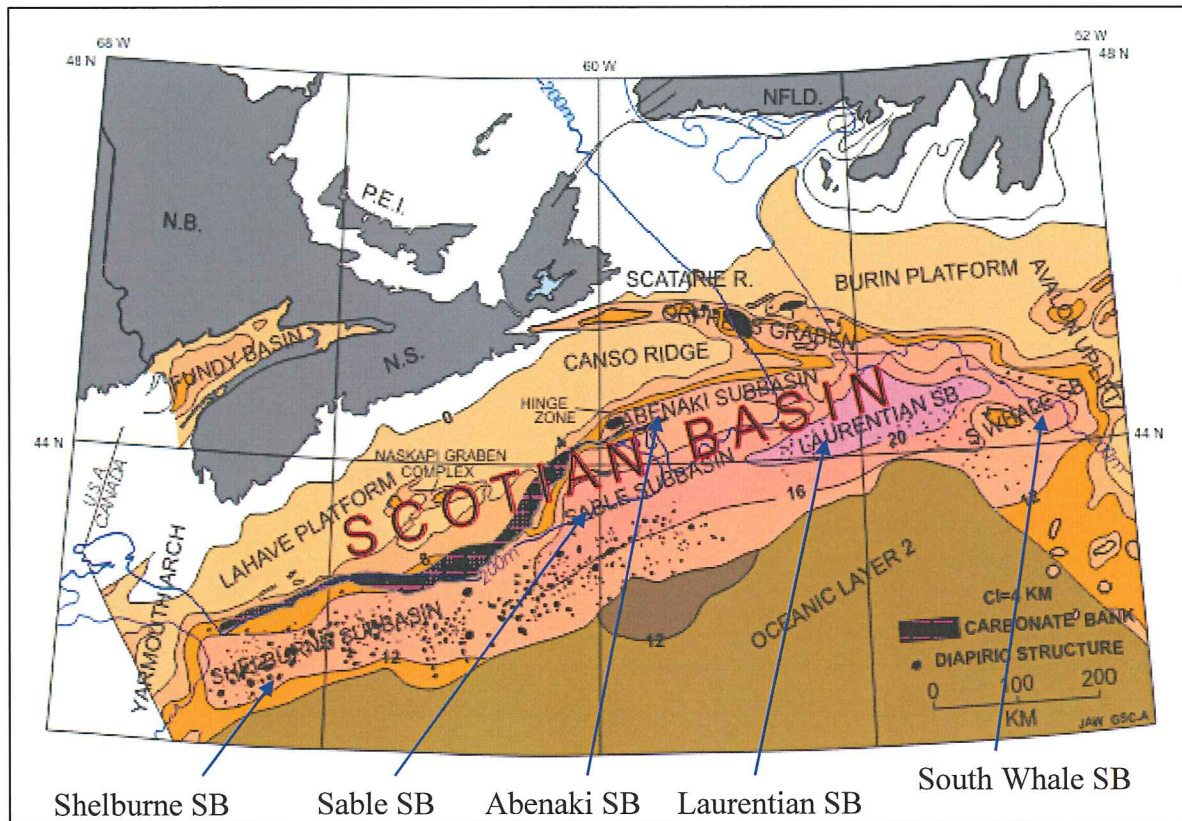
Figure 2.1 – Location Map of the Sub-Basins (SB) that make up the Scotian Basin. (Modified from the Natural Resources Canada web site).

The Scotian Basin is broken into five sub-basins from west to east: the Shelburne, Sable, Abenaki, Laurentian and South Whale Basins (Fig 2.1). These sub-basins experienced prolonged periods of subsidence allowing the accumulation of over 12 km thick of sediments, with a maximum thickness of 18 km (Fig 2.2). The sub-basins that

make up the Scotian Basin were the focus of evaporite deposition during arid climatic conditions and, before these basins uplifted there were thick sequences of redbeds deposited with thin layers of evaporites (Wade and MacLean, 1990).

Sediment distribution varies over the Scotian margin as shown in (Fig 2.2). The Shelburne Sub-Basin located in western portion of the Scotian Margin, has its thickest sediments on the present day continental slope and rise, whereas on the eastern portions of the Margin (Scotian and Laurentian basins) the thickest sediment deposition is found on the outer shelf region (Louden, 2002).
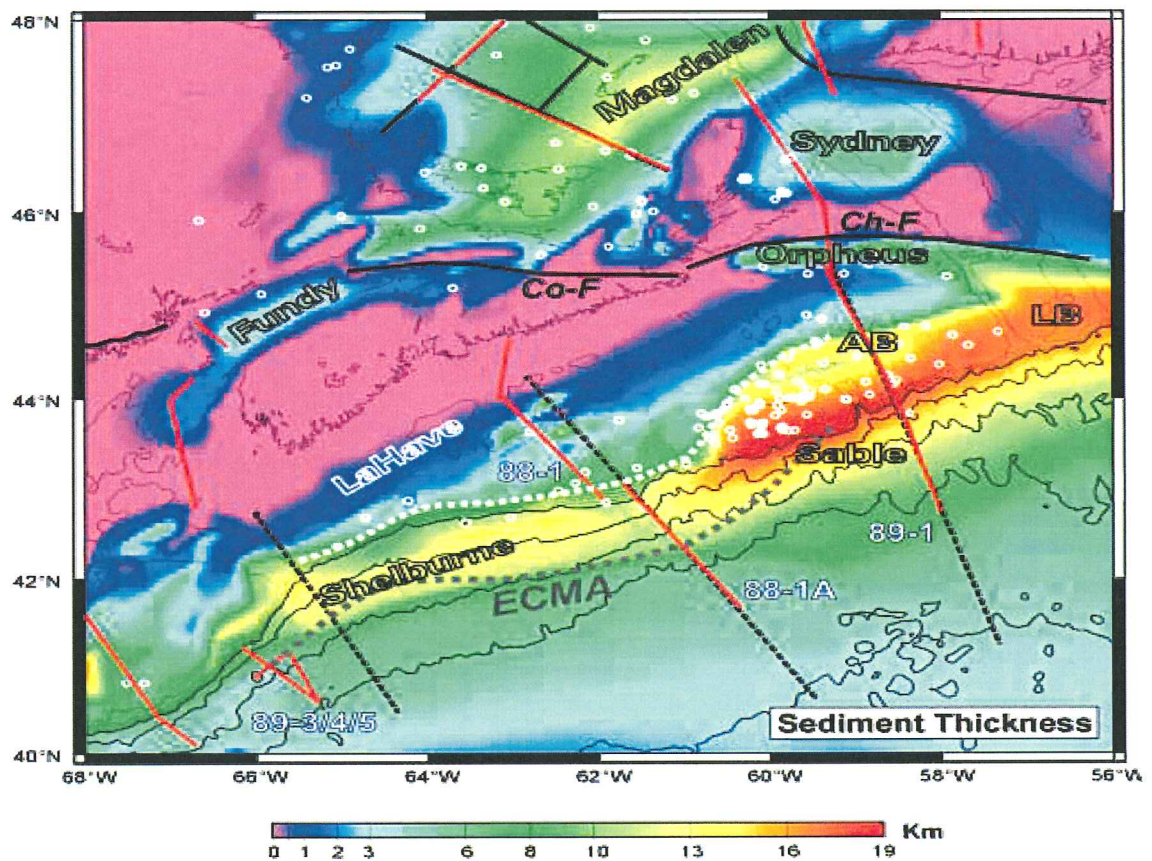
Figure 2.2 – Total sediment thickness map for Nova Scotia. (AB – Abenaki Sub-Basin; LB-Laurentian Sub-Basin; ECMA – East Coast Magnetic Anomaly) Modified from Louden (2002).

7

The Scotian margin has been affected by the mobility of the Argo salt Formation since the Triassic but is otherwise volcanically inactive and seismically stable. Figure 2.3 is a stratigraphic diagram of the Scotian Basin which summarizes the Mesozoic and Cenozoic slope geology (Kidston *et al.*, 2002).
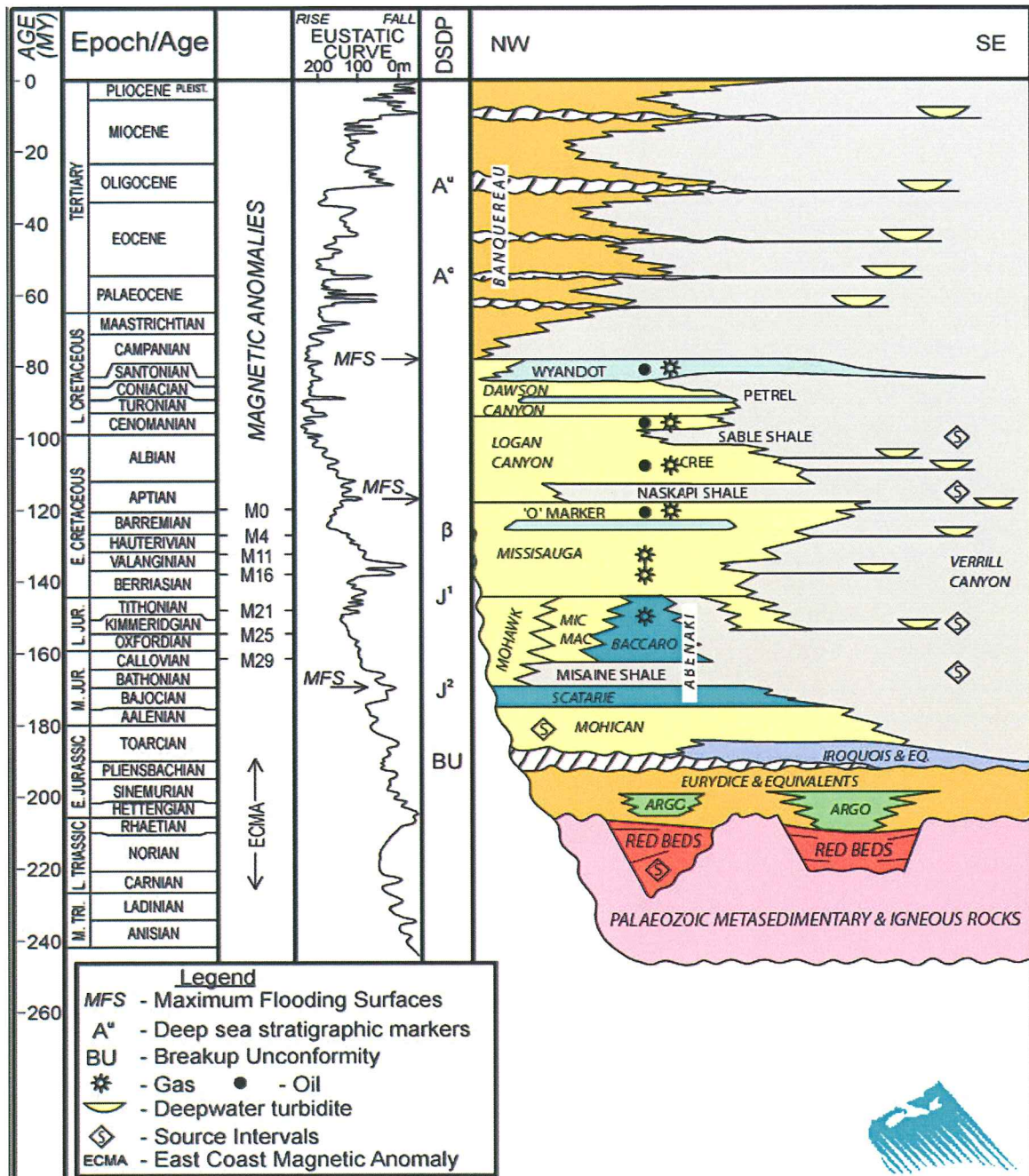
Figure 2.3 – This Diagram displays the stratigraphy and the geology of the Scotian Slope during the Mesozoic and Cenozoic (from Kidston *et al.*, 2002).

2.2 Cenozoic Geology

Piper and Normak (1989) synthesized the late Cenozoic stratigraphy for the south-eastern portion of the Canadian margin. Several marker horizons were identified across the Scotian Slope that correlate with major geologic events. For example, reflector C (Table 2.1) indicates an early Pleistocene lowstand where increased slope incision occurred, with some of these canyons persisting through until the Quaternary. Reflector B (Table 2.1) indicates a change in sedimentation style across the Scotian Slope, associated with the shelf crossing glaciation during the middle Pleistocene (Mosher *et al.*, 2004).

Reflector Name	Regional Reflector*	Probable Age**
Light red	A	
Light yellow		
Brown		
Carmine	B	middle Pleistocene (0.45 Ma)
Gold		
Rose		
Gray	C	basal Pleistocene (1.6 Ma)
Magenta		
Blue		
Red	D	
Lavender	E	middle Pliocene
Orange		
Pink		basal Pliocene
Canary	F	early Miocene (deep water); Miocene/Eocene unconformity (shallow water)

*Regional reflectors correspond approximately to the scheme of Piper and Normark (1989).
**Ages based on Shubenacadie H-100, except for gray, which is based on Acadia K-62.

Table 2.1 – Late Cenozoic Stratigraphy of the Central Scotian Slope (Mosher et al., 2004).

2.3 Seismicity

The Scotian margin and the surrounding regions are found within the stable area of the North America plate. Recorded earthquake activity in this area is low with exception of a single destructive event in 1929. It is estimated that there is an occurrence of 450 earthquakes in Eastern Canada every year with approximately four events having a magnitude larger than four. Thirty events exceeded a magnitude of three. Any seismic event larger then magnitude three that occurs on the East Coast of Canada is recorded by the seismograph network of Natural Resources Canada. Typically within a decade there will be three events larger than magnitude five. Seismic events that occur in the Atlantic Canada region are not well understood since the area is not located on the edge of the North American Plate. It is suggested that the source of seismic activity for this area is a result of regional stress fields where earthquakes are concentrated in areas of crustal weakness. The yearly earthquakes experienced by Eastern Canada typically occur in clusters at depths ranging from the surface to 30 km depth. Earthquakes are not restricted to these areas and can occur anywhere in Eastern Canada (NRCAN). Figure 2.3 shows the frequency of earthquakes from 1600 to present day that have occurred along the Scotian margin and Laurentian area. Seismicity on the Scotian margin is not focused to any particular area with events being recorded from the Northeast Channel to the Grand Banks off Newfoundland.
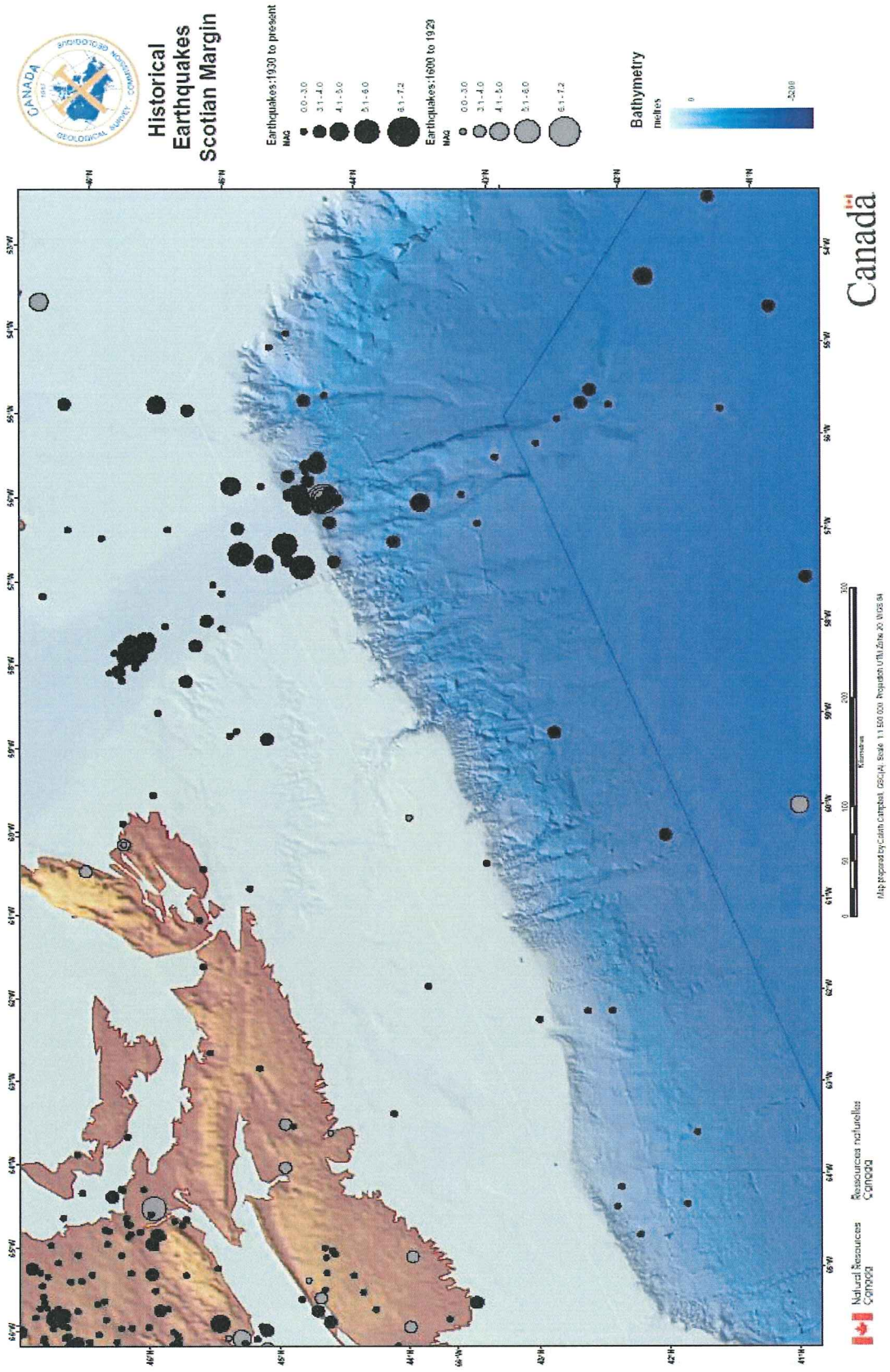
Figure 2.4 – Seismicity map of Nova Scotia and surrounding areas with earthquakes since 1600 to present day. From Adams and Halchuk, 2003.

11

2.4 Glaciation

During the Tertiary, the Scotian margin experienced major episodes of sea level lowstands (Piper and Normak, 1989) which resulted in the basinward progradation and accumulation of prodeltaic shales and large scale canyon incisions along the outer Scotian Shelf and Slope. When terrestrial glaciation occurred during the Pleistocene, an increase in the rate of sedimentation developed on the Laurentian Fan and Scotian Slope. Also during the Pleistocene, large scale incision took place along the Scotian Slope, but the depositional environment remained prodeltaic (Mosher *et al.*, 2004). Since the first glacier shelf crossing, which took place 0.5 Ma (mid-Pleistocene), proglacial sediment deposition has dominated the continental slope. With changing ice margin advances and retreats during the Pleistocene, the sedimentation rates and processes also varied accordingly. Rapid deposition of proglacial sediments occurred during glacial advances and retreats, whereas slow sediment deposition occurred during sea level highstands (Mosher *et al.*, 2004). Periods of instability on the Scotian Slope roughly correlated to episodes of rapid deposition during de-glacial stages (Mosher, 1987).

The Late Wisconsinian glaciation was the last glacial stage to affect the Atlantic continental margin with its final retreat off the Scotian Shelf beginning ~ 16000 BP (Fig 2.5) (King and Fader, 1986). The rate of post-glacial sedimentation on the Scotian Slope has slowed due to the Holocene increase in sea level (Fig 2.6), sedimentary processes being dominated by pelagic and hemipelagic deposition (Mosher *et al.*, 2004).

Figure 2.5 – The extent of the ice sheet before the beginning of its retreat 16000 BP (from Shaw and Courtney, 2002).
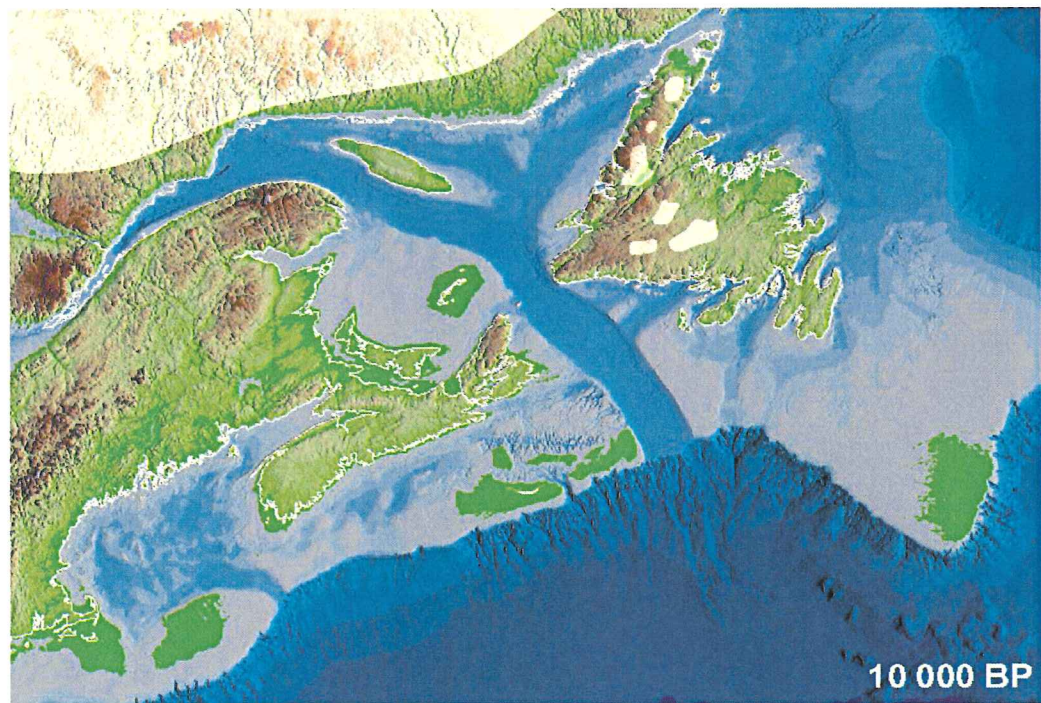
Figure 2.6 – The height of sea level and how far the ice sheet retreated at the beginning of the Holocene (from Shaw and Courtney, 2002).

2.5 Physiographic and Stratigraphic Features

2.5.1 Stratigraphy

During the Miocene and the early Pliocene thick layers of shales were deposited on the Scotian Slope. By mid Pliocene, the continental slope was incised by channels suggesting periods of lower sea level with delta progradation across the continental shelf. Sedimentation was dominated by lowstand deltaic sedimentation. During the middle Quaternary the first ice sheets crossed the Scotian Shelf. The eastern the Scotian Slope deep canyons and valleys were cut by sub-glacial meltwater with proglacial suspended sediment accumulating in the inter-valley areas. The chronology for the Pliocene is provided by ties to wells while most of the chronology for the Pleistocene is only available by extrapolation (Piper).

2.5.2 Gas Hydrates

Gas hydrates are stable at specific temperatures and pressure conditions. They are found therefore in two principal areas: underground at higher latitudes where surface ground temperatures are less then $0°$ C (ie. permafrost regions) and oceanic continental slope and rise sediments where hydrostatic pressure is high (>3 MPa). Gas hydrates are found offshore between subsurface depths of 300 and 500 m; the depth-determining factor typically being the subsurface temperature gradient. Gas hydrate is an ice-like substance with water molecules arranged in a rigid framework of cages. These cages encompass molecules of gas, typically methane (Kvenvolden, 1999). Gas hydrates form through microbial or thermogenic processes (Kvenvolden et al., 1993).

When there are changes in the pressure/temperature field, gas hydrates will begin to dissociate from a solid to a gas, expanding 64 times of its original size. It is this source

of gas, which is the potential rapid release of gas, which theoretically could cause a mass failure by increasing the pore pressures and thereby reducing the shear strength (Kvenvolden *et al.*, 1993).

It is difficult to recognize gas hydrates in formation. One of the few methods to recognize gas hydrates is the identification of bottom simulating reflections (BSRs) marine seismic records. A BSR is defined as "an anomalous, high-amplitude, negative-polarity seismic reflection that sub-parallels the seafloor bathymetry at subbottom depths between 300 and 500 m" (Kvenvolden et al., 1993). The BSR represents free gas trapped below the base of the gas hydrate, therefore approximately representing the base of the gas hydrate stability zone. When pressures increase or the thermal gradient changes, the base of the hydrate shifts (Kvenvolden et al., 1993). Figure 2.7 displays the stability zone of gas hydrates along the Scotian margin.
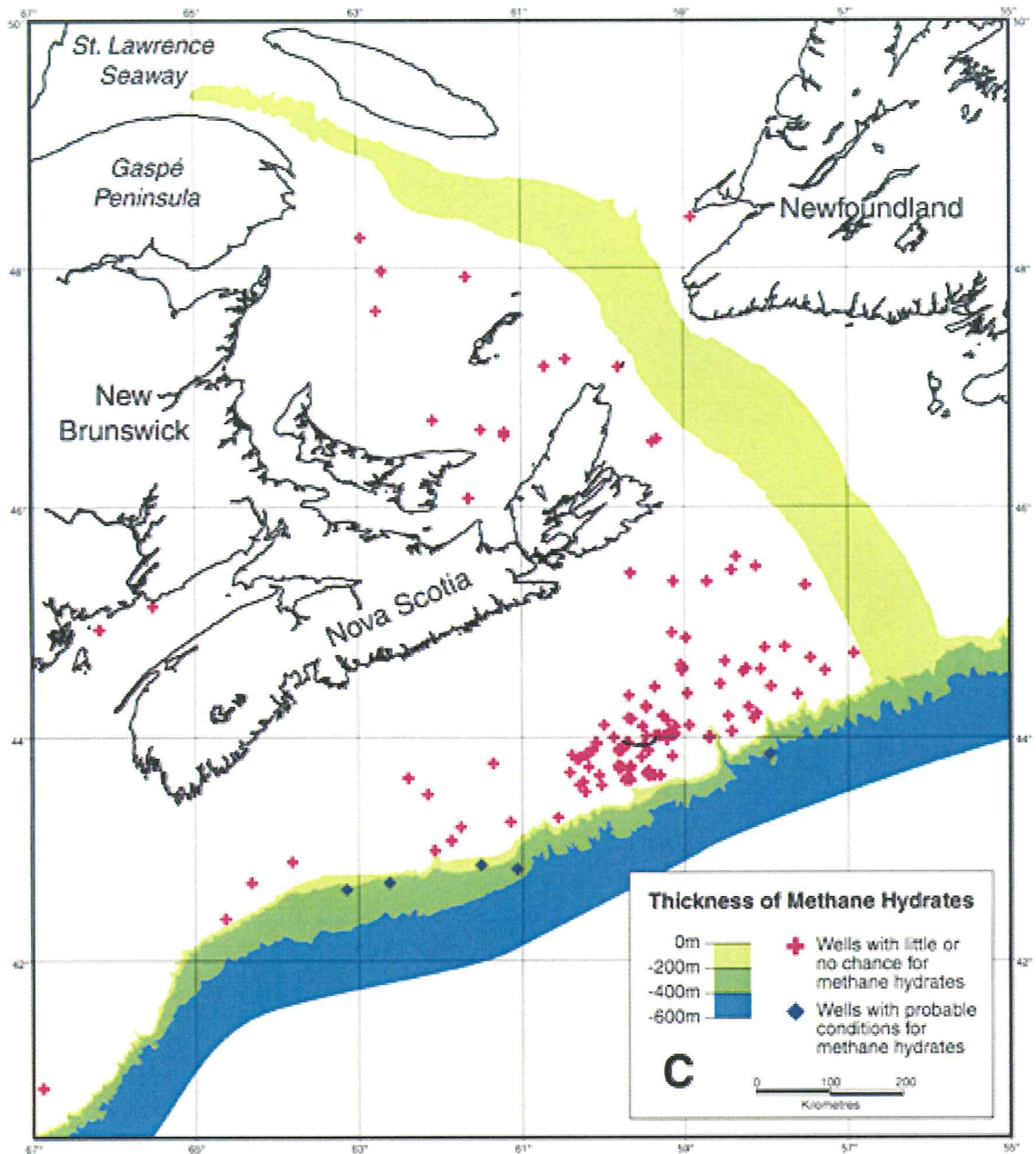
Figure 2.7 - A map displaying the stability zone of gas hydrates along the Scotian margin (from Majorowicz and Osadetz, 2003).

16

2.5.3 Salt Tectonics

The Scotian Sedimentary Basin was, and continues to be, affected by salt tectonism, similar to the Gulf of Mexico and some parts of the West African Margin. Due to the physical characteristics of evaporites, evaporitic rocks are much weaker than the sedimentary rocks around them. This property of evaporites increases their mobility under pressure and allows it to deform, creating complexes seen in passive continental margin basins underlain by salt deposits. These passive margins are characterized by a seaward thinning sediment wedge, which is a result of sedimentation from onshore regions. Sedimentary basins influenced by salt tectonics typically have landward extensional faulting accommodated by seaward contractional faulting and folding. This scenario may account for the failure of the sedimentary overburden, which accompanies the flow of the underlying salt (Gemmer *et al.*, 2004).

The Argo Formation found under the majority of the Scotian Basin has been dated through the use of spores as being Hettangian in age. The Argo Formation is made up of two different evaporites identified from bore hole data. The Argo F-38 well in the Orpheus Graben displays a finely crystalline dolomite overlain by a massive white and purple, coarsely crystalline, halite with several shale interbeds. Typically, the halite is colourless to light orange and contains beds of red shales. Of all the wells drilled offshore Nova Scotia, only two wells in the Scotia Basin penetrated undeformed, autochthonous evaporates: the Eurydice P-36 well in the Orpheus Graben and the Gloosap C-63 well in the Mohican Graben (Shimeld *et al.*, 2004).

Chapter 3: Methods of Seismic Acquisition and Processing

3.0 Seismic Reflection Principles

Reflection seismics originates with an acoustic source pulse that creates an expanding wave front. When the wavelet interacts with an acoustic impedance interface, some of the energy of the wave is reflected and transmitted. The amount of energy reflected is directly related to the magnitude of the impedance change. There are two aspects of the reflected energy recorded by the receivers at the surface: 1) the time it takes for the energy to travel to the reflecting surface and then back to recorder and 2) the strength of the reflected energy (Hart, 2000). The travel time for the energy to travel from the surface to the reflecting horizon and then back to the surface is known as two way travel time (TWT) (Hart, 2000).

3.1 Seismic Data Acquisition

This thesis is based upon study of the Barrington 3D seismic cube. It was acquird in 2001 by the vessel M/V Geco Searcher owned by Den Helder Support Services BV based in the Netherlands. The size of the area covered was 1790 sq. km with a sailing distance of 3978 km. In total 98 lines were shot in water depths between 660 m to 2200 m. The Barrington data were supplied by the EnCana Corporation.

Marine seismic data acquisition requires three main components: a source, receiver and recorder (Fig 3.1). The source is an instrument or device that creates acoustic energy, usually near the surface of the ocean. The sound energy travels through water column and through the subsurface sediments. Some of the acoustic energy created by the source is reflected off the seafloor and other impedance surfaces below the seafloor. The acoustic source in this study is a 260 cu. in. air gun array. Air is

pressurized in the chambers of the airgun. It is released suddenly creating an expanding bubble and pressure wave. These pressure waves have acoustic energy with peak frequency of 70 hertz and band width of 5 – 100 hertz in this studies data set. The receiver, which is a string of hydrophones towed behind the survey ship, converts the pressure signal of the sound waves from the source into a voltage electrical signal, which is then digitized and recorded.
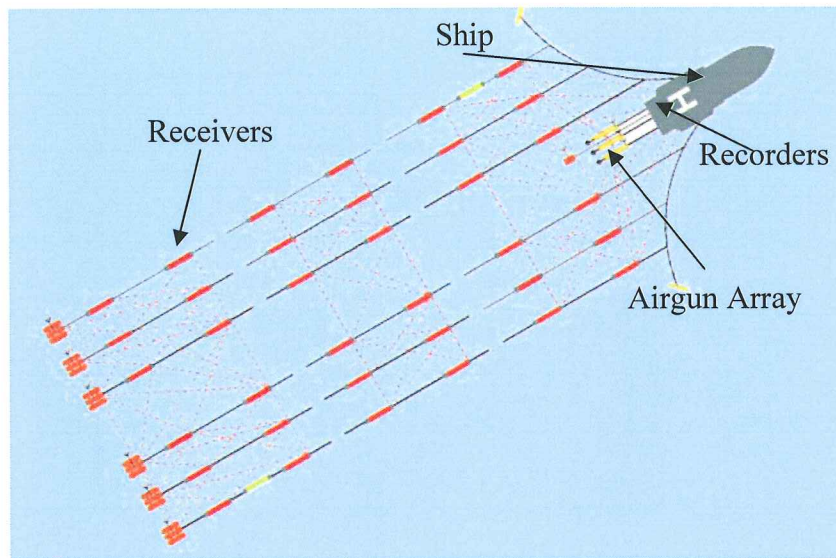
Figure 3.1 – Schematic of seismic acquisition by a ship. (Modified from www.acsonline.org/issues/sound/images/seismicShipConfig.jpg).

3.2 Source

The Barrington data were collected using Bolt long life air guns, models 1500LL and 1700X11. The seismic lines were shot in a 56.5° and 236.5° grid with a line spacing of 450 m. The M/V Geco Searcher towed two air gun arrays with each array having three sub arrays with eight metre spacing. The arrays had 20 air guns each with a spare 260 cu. in. cluster in the center. The operating pressure for each array was 2000 psi with the total volume of 3784 cu. in. per array. The air gun arrays were towed at a depth 6 m. The shot

point interval for these air gun arrays was a 30.0 m flip-flop with the starboard sources firing in odd shots. The air guns produced a peak/bubble ratio of 24.2.

3.3 Receiver

The M/V Geco Searcher towed six multi-channel streamers with an active length of 6000 m each. Each streamer consists of 240 channels with the near trace being 1 and the far trace being 240. The channels are in intervals of 25 m. The streamers are constructed in 60 sections with each section being 100 m long with four groups per section of 2 X 12.5 m. The streamers are towed at a depth of 8 m with up to1.5 m of travel in the vertical direction.

3.4 Recorder

Shot data were recorded for11 seconds at a sample rate of two ms. The data are formatted in De-multiplexed SEG-D 8015 Rev. 2 with a LC Filter set at 3 Hz, 18 db/octave and a HC Filter 180 Hz, 70 db/octave. The data are recorded on De-multiplexed 3-M Blackwatch 3590 HPT tape cartridges with 10 GB of space.

3.5 Processing

The original SEG-D data were reformatted to SEG-Y. Next the seismic data were merged with the Radio-navigation data. Spherical divergence compensation was applied to the data along with signal preserving attenuation of random noise. A F-K filter was the applied followed by a source-receiver delay compensation and deterministic deconvolution. The seismic data was then sub-sampled to four ms where a velocity analysis, a normal move out (NMO) and RAMUR multiple attenuation was applied. Multiple attenuation is applied to the data to remove the seafloor multiple from the useable data. Seafloor doubles occur when for example, if the seafloor is reached at 1.0

seconds and the data reflects up to 5.0 seconds, at the 2.0, 3.0 and 4.0 second intervals a reflection of the seafloor will appear. The data then went through static binning, dip moveout (DMO), missing trace interpolation, velocity analysis and RAMUR multiple attenuation mute. An alpha trim stack of 75% is applied to the data followed by a K5 notch filter, and x-line interpolation to 12.5 m. The product of these sets then is put through a migration with 97% smoothed DMO velocities and a time-varying filter from the water bottom. After the data went through Dynamic equalization it was exported as SEG-Y data.

3.6 Navigation

The navigation used onboard the M/V Geco Searcher to acquire the Barrington data was a Geco TriNav GPS with Osiris Veripos-I using reference stations in St. John's and Halifax with augmentation data provided by Veripos. The primary geodetic datum used in this project was the World Geodetic System 1984 (WGS-84). The projection used was the Universal Transverse Mercator (UTM) with the work being done in UTM Zone 20 West.

3.7 Seismic Horizon Picking Parameters

The Barrington 3D data cube was loaded into the SMT Kingdom Suite software for interpretation. The seismic horizons are picked by the peak of the wavelets using through the auto-fill option. The data cube consists of cross-lines and in-lines and horizons were on every 20th seed line. After manually picking, a polygon hunt can be performed to infill horizons on all other traces.

Chapter 4: Results

4.1 Introduction

The seismic data presented in this chapter is from the Barrington 3D cube and is described by seismic stratigraphy and facies analysis.

4.2 Seismic Facies Analysis

A seismic facies unit, as defined by Sangree and Widmier (1979) is "a mappable group of reflections, whose elements, such as reflection pattern, amplitude, continuity, frequency, and interval velocity, differ from the elements of adjacent units". Through the use of seismic facies analysis, the geometry of the unit, the depositional environment and processes, and the direction of sediment transport can be interpreted. Several terms are used in seismic facies analysis to describe reflection geology such as; parallel, sub-parallel, wavy, divergent, convergent, chaotic, incoherent, concordant, high amplitude or low amplitude (Sangree and Widmier, 1979).

Within the Barrington 3D cube, four different seismic facies were identified as Facies A, B, C and D (Fig 4.1). Facies A comprises continuous, parallel to wavy, high amplitude reflectors which are easy to correlate and identify across the study area. Facies B consists of discontinuous, moderately high amplitude incoherent reflectors which are not laterally continuous. Facies C consists of low amplitude incoherent reflectors which can not be easily correlated distance. Facies D consists of continuous, parallel to wavy, low amplitude reflectors. The nature of the low amplitude reflectors make it difficult to identify across the study area.
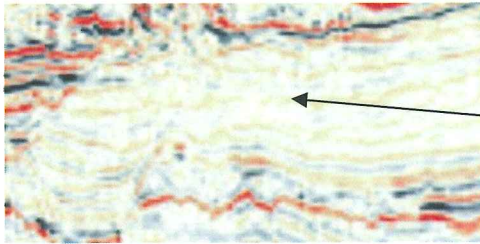
Facies A – continuous, parallel to wavy, high amplitude reflectors
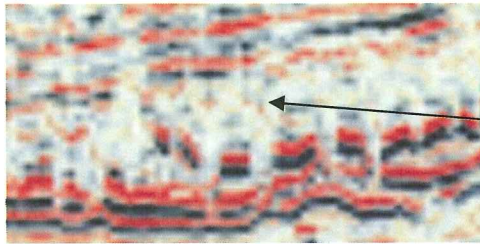
Facies B – discontinuous, moderately high amplitude incoherent reflectors
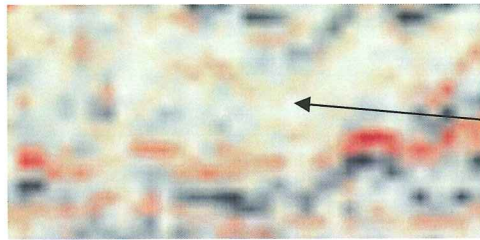
Facies C – discontinuous, low amplitude incoherent reflectors
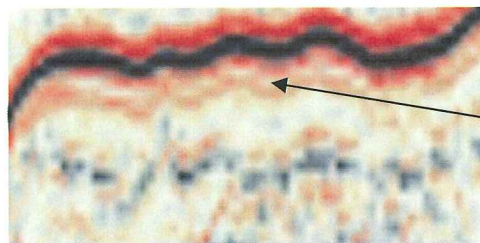
Facies D – continuous, parallel to wavy, low amplitude reflectors

Figure 4.1 – Characteristics for Seismic facies A, B, C, and D.

4.3 Seismic Horizons and Reflectors

Eight seismic reflection horizons were chosen and correlated throughout the study area. They were chosen on the basis of strong coherency and wide spatial distribution and form boundaries between depositional units. The eight horizons identified have been used to separate the six units identified within the study area. Each of the eight horizons is either the top or base of one of the units. The units are described according to their seismic facies and how that facies is distributed within the unit. These units are defined by their bounding surfaces; for example the Red-Royal Blue unit refers to the area confined between the red and royal-blue horizon. Figures 4.2 and 4.3 show strike and dip profiles respectively which display the observations within the units. The units within the Barrington Cube from oldest to youngest, are red-royal blue, royal blue-orange, orange-green, green-yellow, blue-aqua blue, and yellow-yellow (seafloor) (Table 4.1).

| **Table 4.1** – Seismic Units and their bounding colored reflectors horizons from youngest to oldest.	Units	Bottom Boundary	Top Boundary
	Unit 1	Yellow Reflector	Yellow (seafloor)
	Unit 2	Blue Reflector	Aqua Blue Reflector
	Unit 3	Green Reflector	Yellow Reflector
	Unit 4	Orange Reflector	Green Reflector
	Unit 5	Royal Blue Reflector	Orange Reflector
	Unit 6	Red Reflector	Royal Blue Reflector

Figure 4.2 and 4.3 are two seismic lines from the Barrington 3D data cube with the horizon's found in Table 4.1 displayed on the seismic lines. Figure 4.2 is inline 2491 of the Barrington Cube and is orientated strike to the Scotian Slope. Figure 4.3 is cross-line 2707 and is orientated dip to the Scotian Slope. Both figures have a horizontal scale of 1200 m. Figure 4.4 is map displaying the location of the seismic lines used to illustrate each seismic facies.
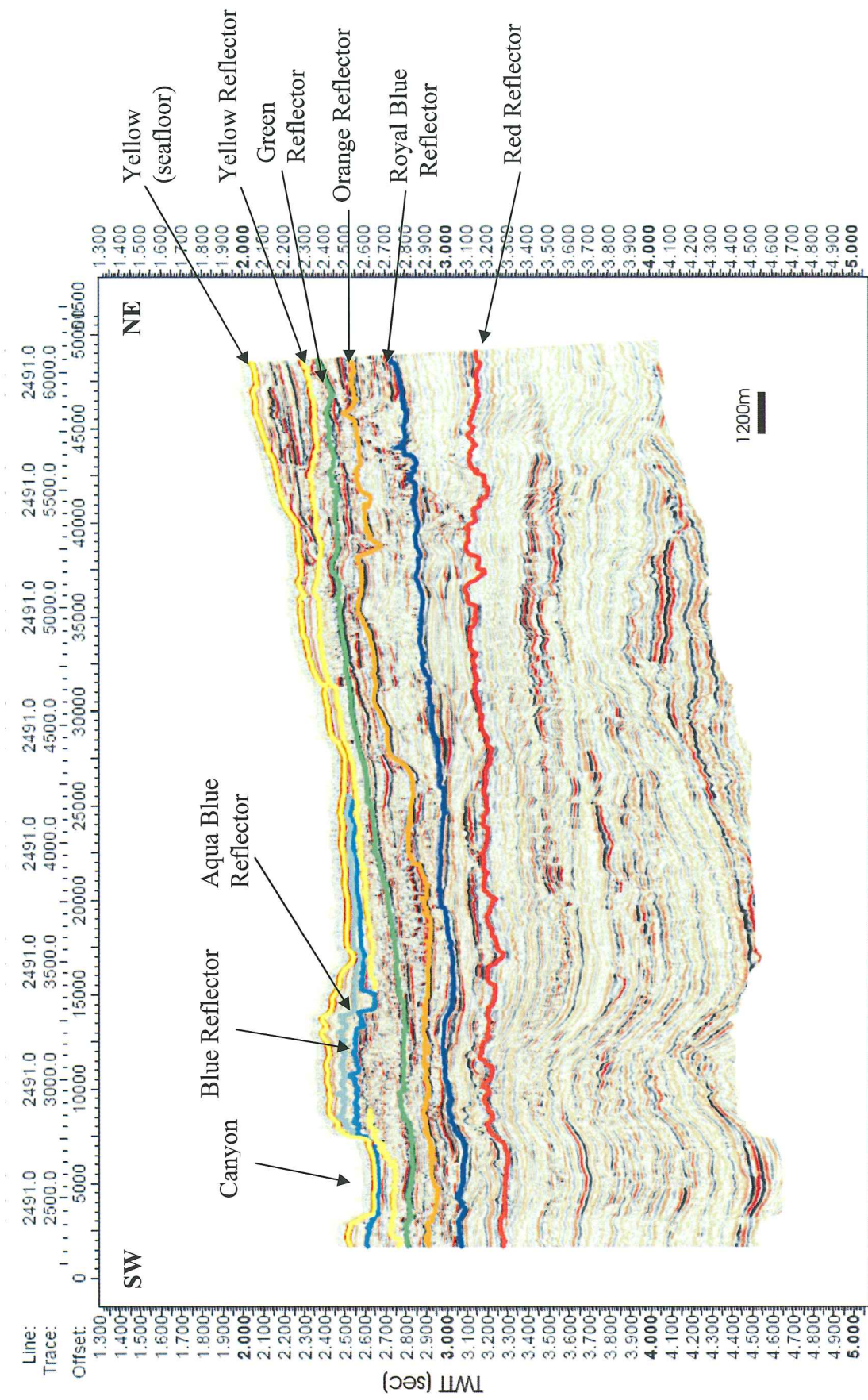
24

Figure 4.2 – Strike line 2491

25
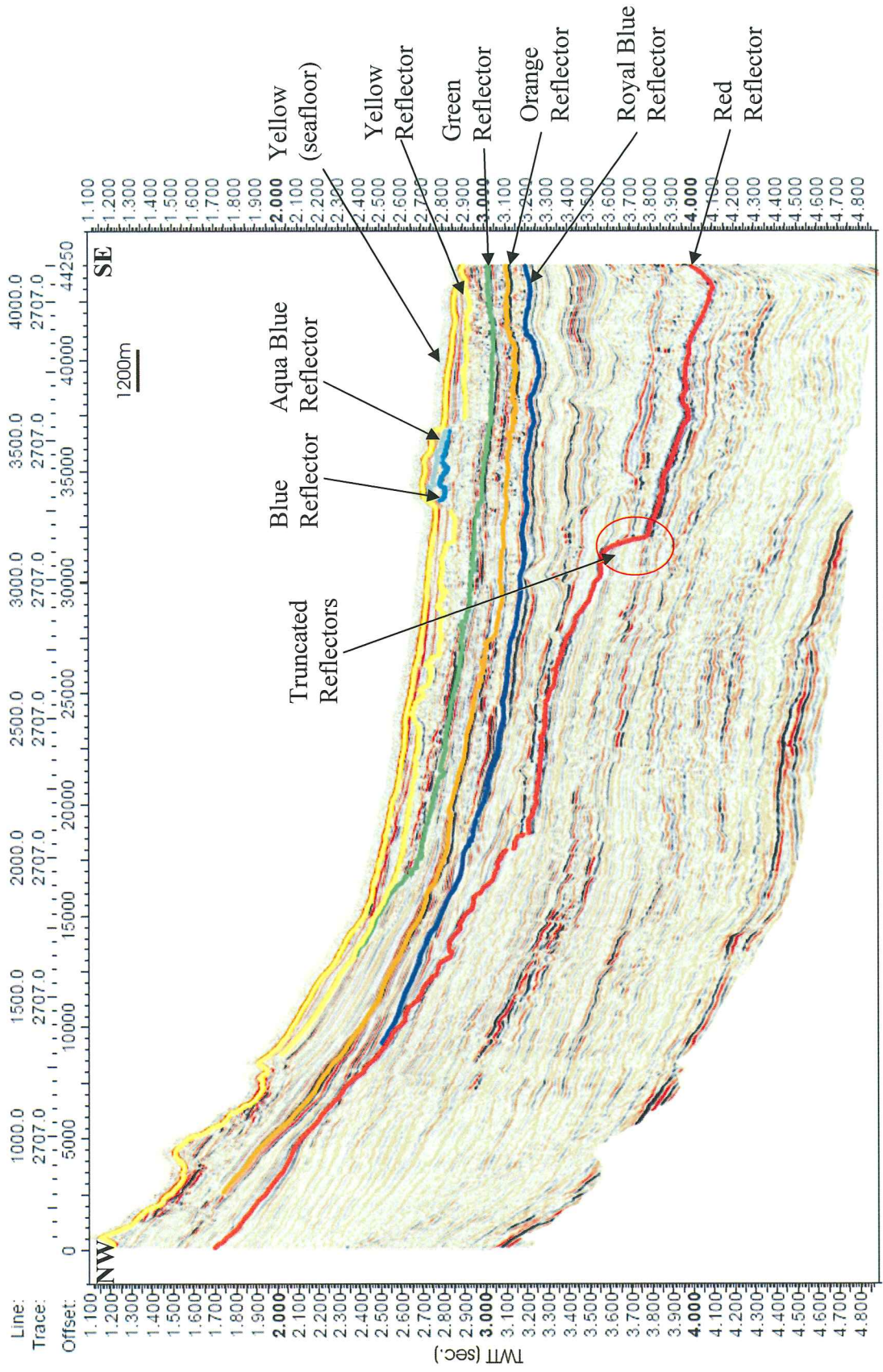
Figure 4.3 – Dip line 2707
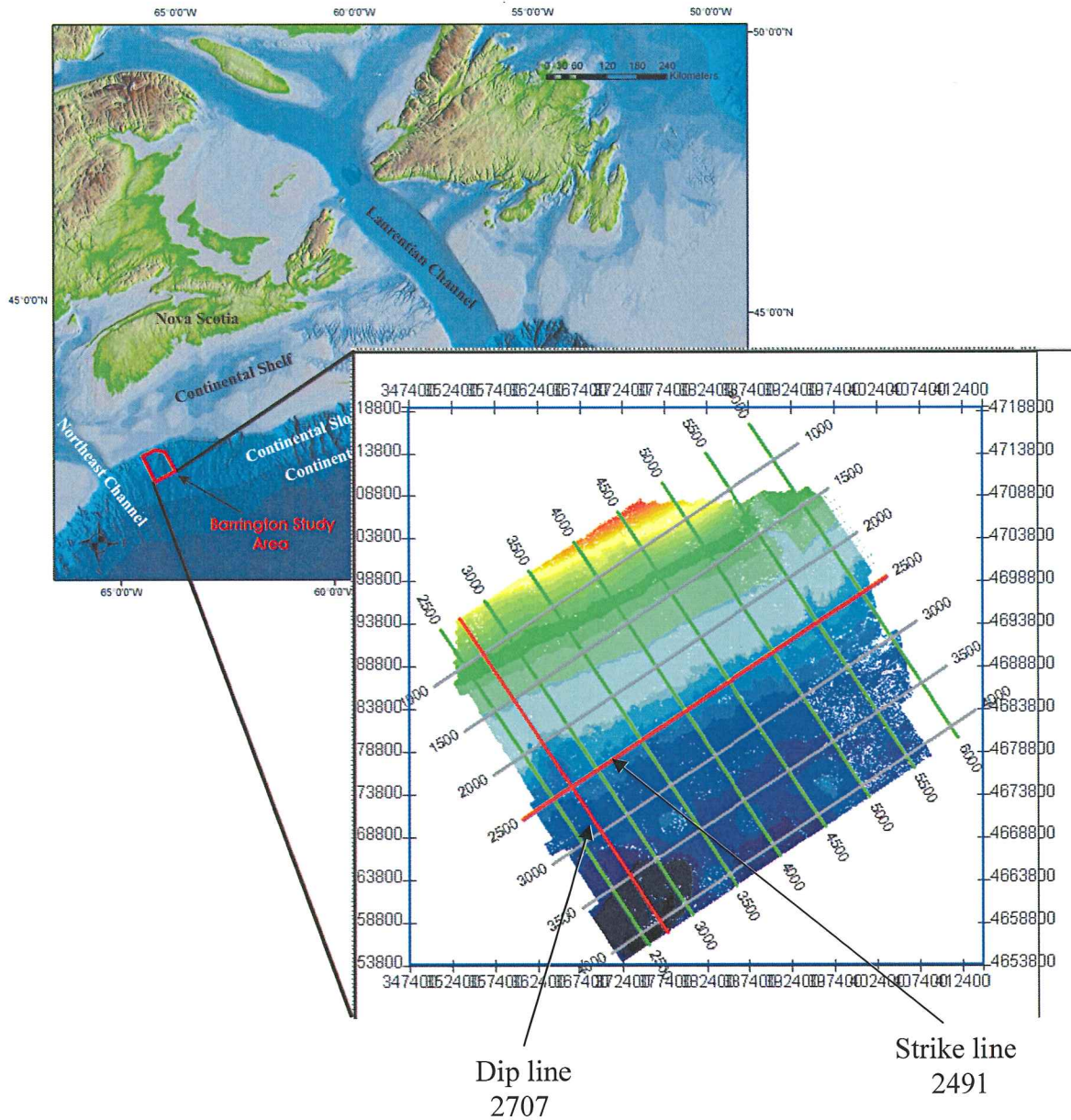
Figure 4.4 – Location map of the strike line 2491 and dip line 2707 within the Barrington cube.

4.3.1 Red-Royal Blue unit

The Red-Royal Blue unit marks the base of the data examined in the Barrington study area. The red and royal blue reflectors are moderate to high in amplitude and are easily correlated across the study area as seen in Figure 4.5. This package of sediment is dominated by Facies A containing wavy reflectors that terminate against other reflectors. The unit thickens from 190 milliseconds (ms) in the southwest to 430 ms in the northeast. Morphologically there are several small scale "V" shaped erosional features.

4.3.2 Royal Blue-Orange unit

The Royal Blue-Orange unit overlays the Red-Royal Blue unit and can be correlated across the study area as shown in figure 4.6. This package is composed mostly of mostly Facies A, but some areas are dominated by Facies B and Facies D. The parallel to sub-parallel reflectors in this unit converge and diverge in the southwest-northeast direction across the data set where some are truncated by the orange reflector. The unit is similar to the lower unit thickening from southwest to the northeast by 50 ms.

4.3.3 Orange-Green unit

The Orange-Green unit overlays the Royal Blue-Orange unit and is correlated across the study area as shown in figure 4.7. This package is dominated by Facies B with small areas composed of Facies A. This unit remains a constant thickness across the study area at roughly 100 ms. Morphological features in the unit include one "V" and one "U" shaped erosional feature on the northeast end of the data set.

4.3.4 Green-Yellow unit

The Green-Yellow unit overlays the Orange-Green unit and is correlated across the study area as shown in Figure 4.8. This package is dominated by Facies B with areas

in the southwest portion of the data consisting of Facies A. This unit has consistent thickness of 60 ms with one 2400 m section in the southwest end that has a thickness of 180 ms.

4.3.5 Blue-Aqua Blue unit

The Blue-Aqua Blue Unit overlays the Green-Yellow unit but is not continuous across the study area as seen in figure 4.9. This unit is found within the Yellow-Yellow (seafloor) unit and is laterally extensive for 7200 m. Unit 2 is dominated by Facies C and pinches out towards the northeast. There is one "U" shaped erosional morphological feature which cuts the Yellow reflector.

4.3.6 Yellow-Seafloor unit

The top of the Yellow-Seafloor unit is the seafloor pick with the base being continuous across the study area except for a 2400 m section in the southwest end of the data. This package of sediment is dominantly Facies D with 2400 m in the northeast end being primarily Facies A.
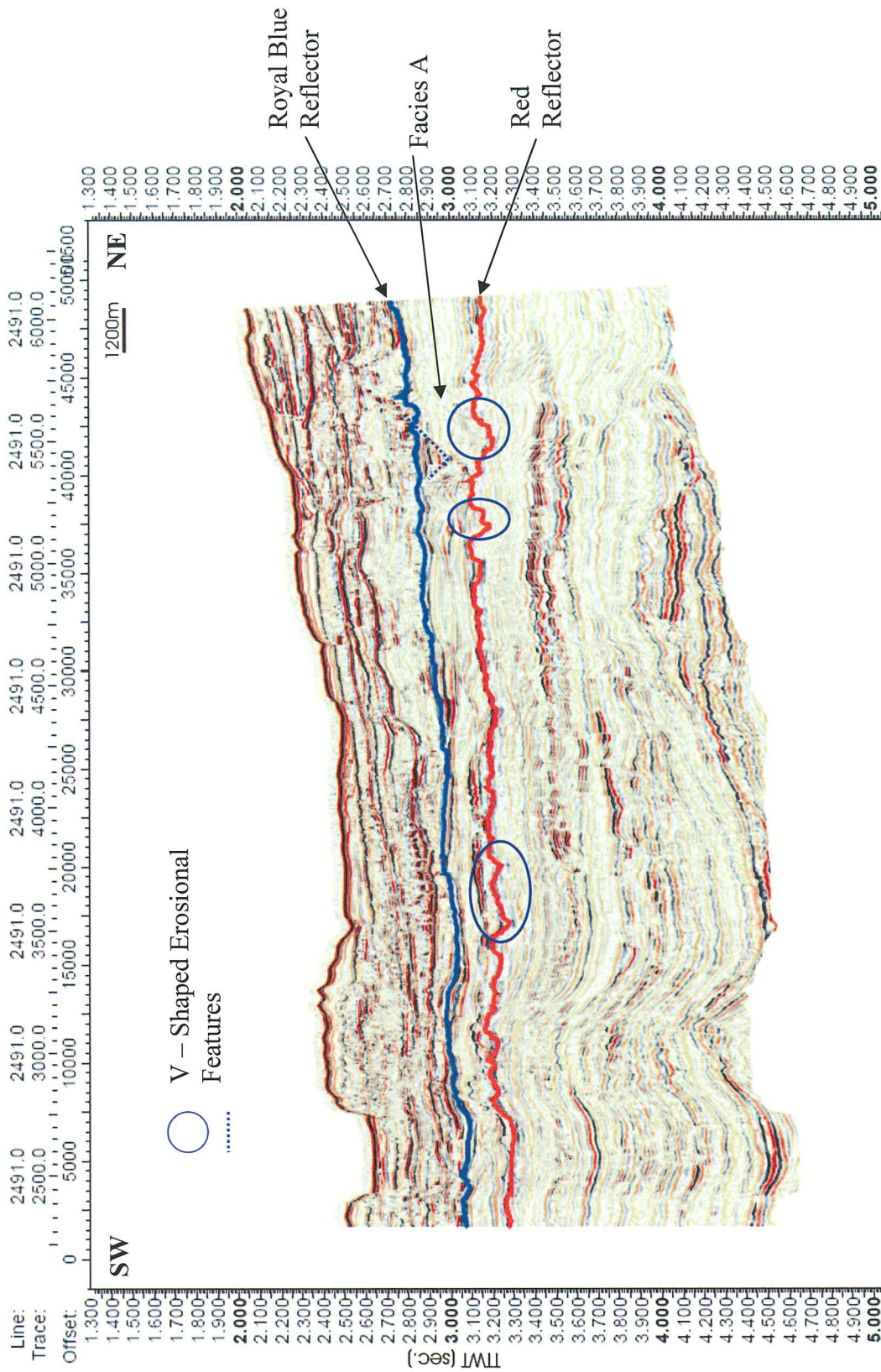
Figure 4.5 – Red-Royal Blue unit seen in Strike line 2491
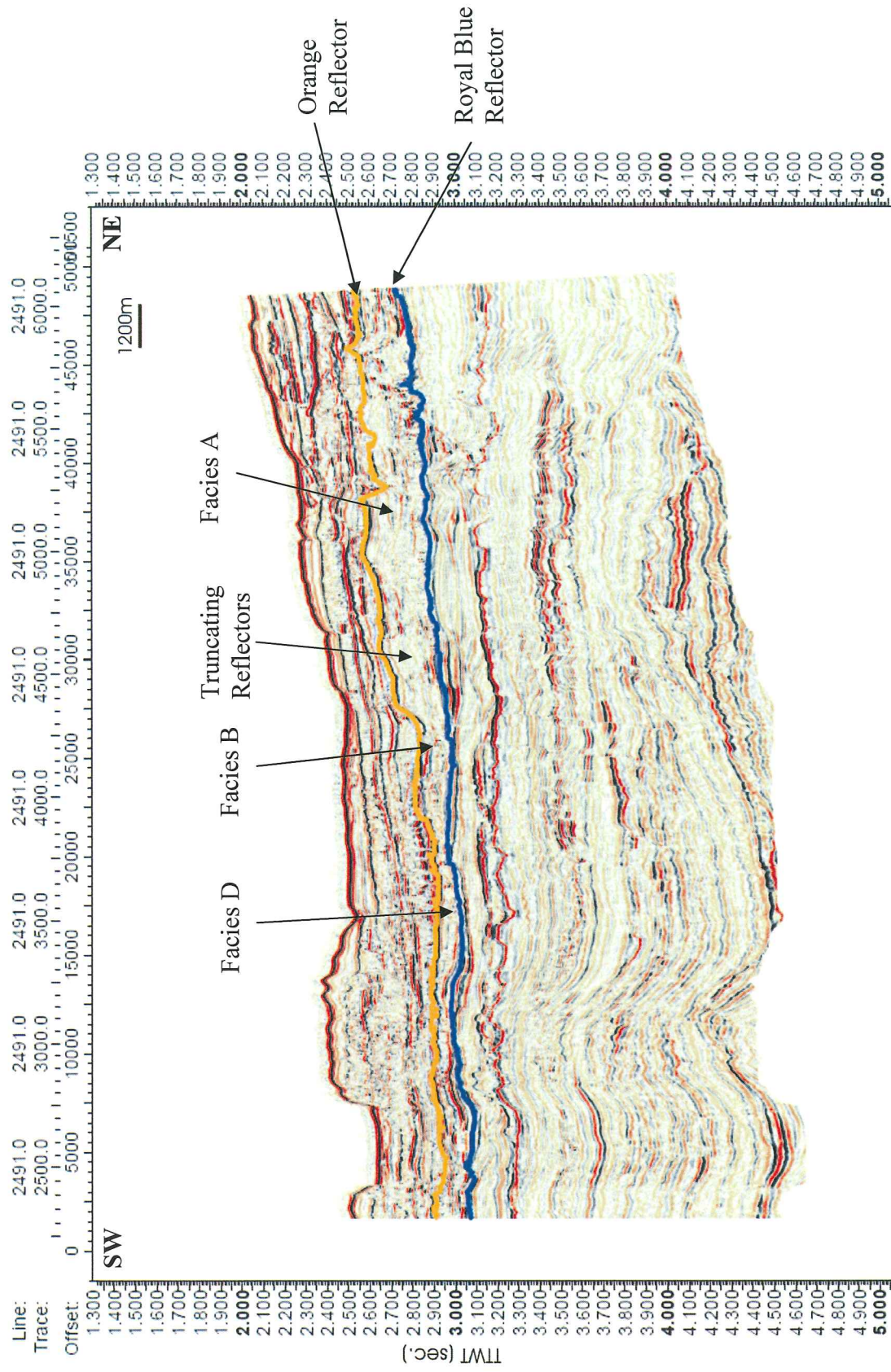
Figure 4.6 – Royal Blue-Orange unit seen in Strike line 2491
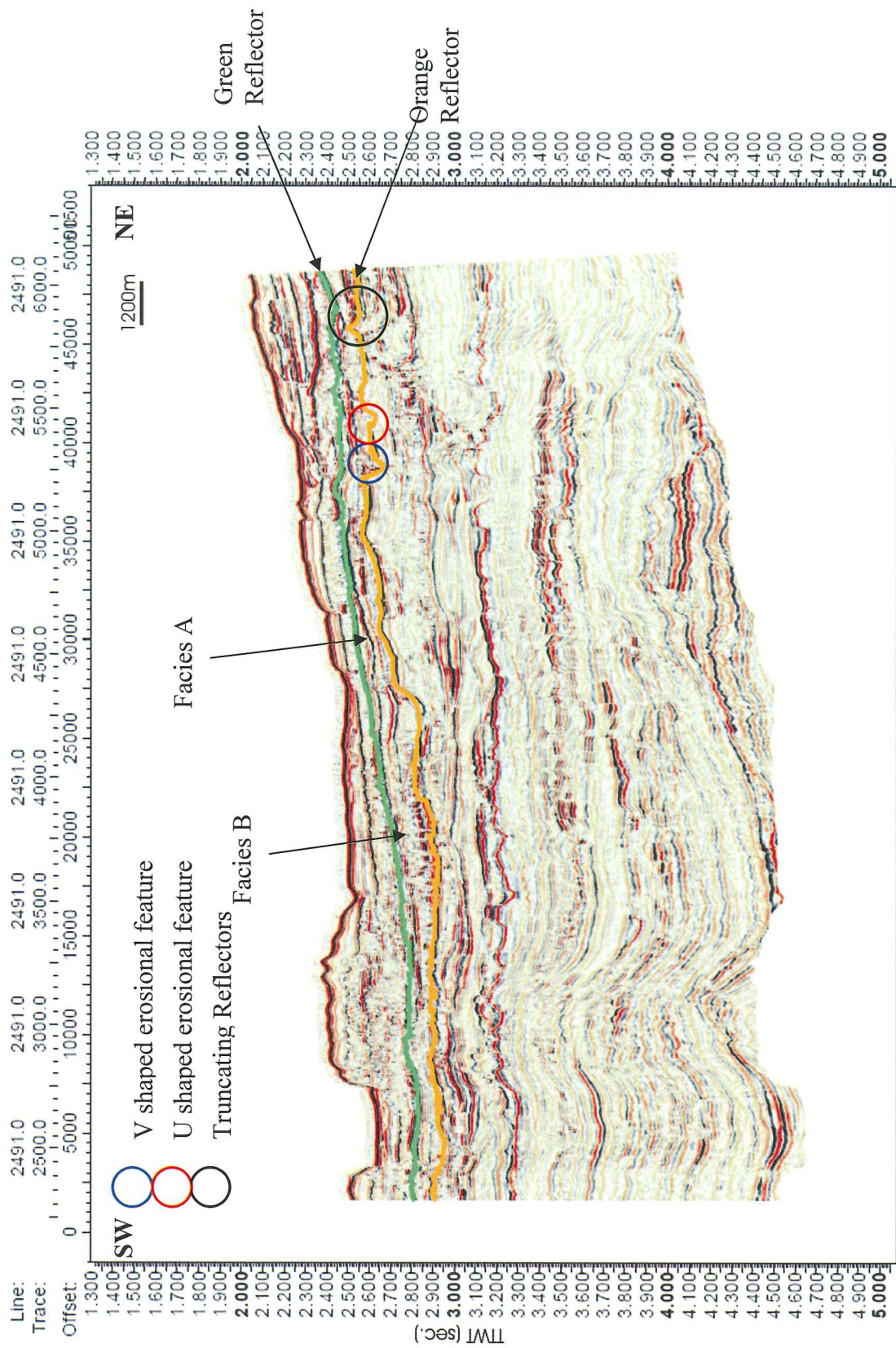
Figure 4.7 – Orange-Green unit seen in Strike line 2491
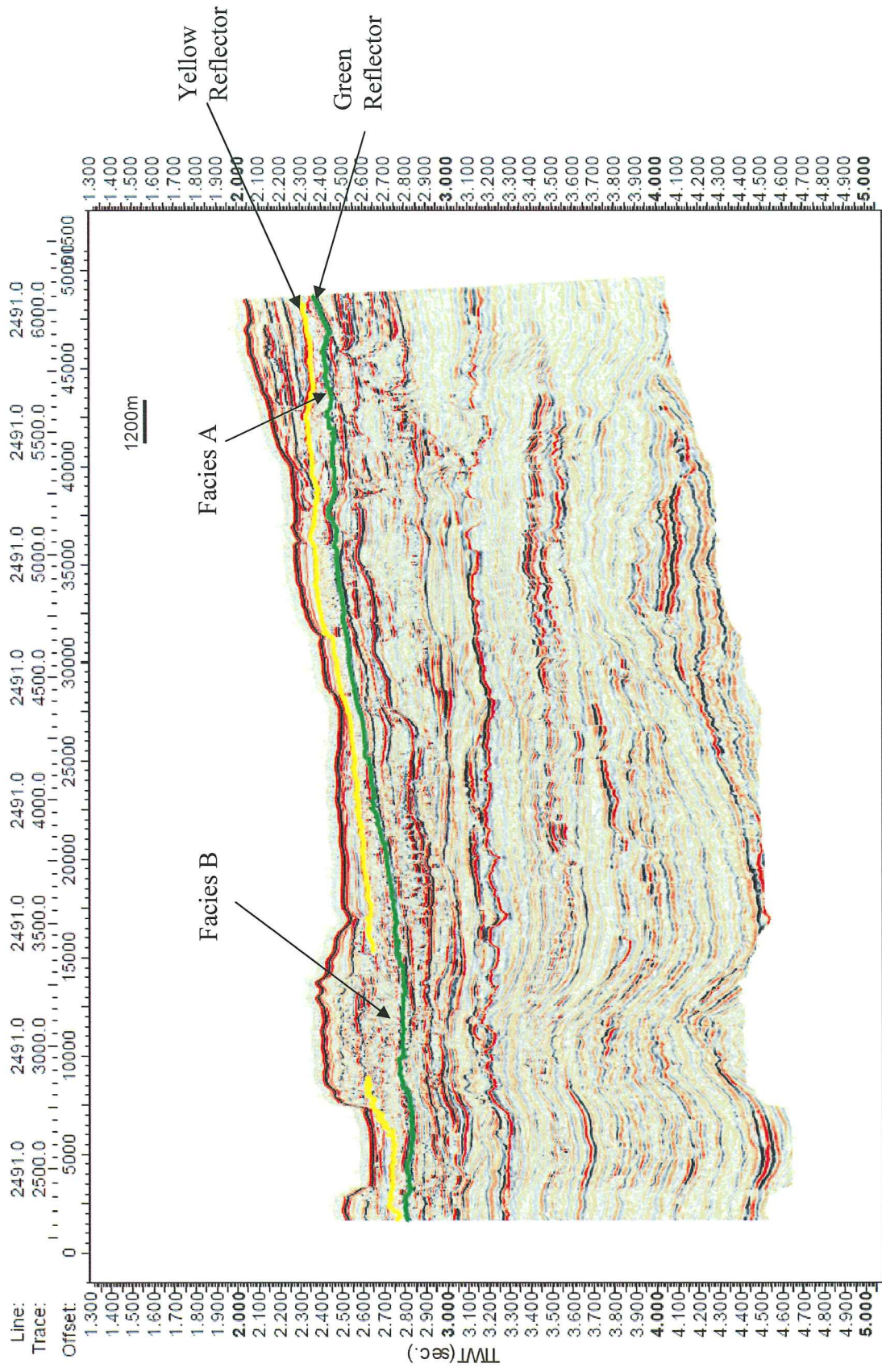
Figure 4.8 – Green-Yellow unit seen in Strike line 2491

33
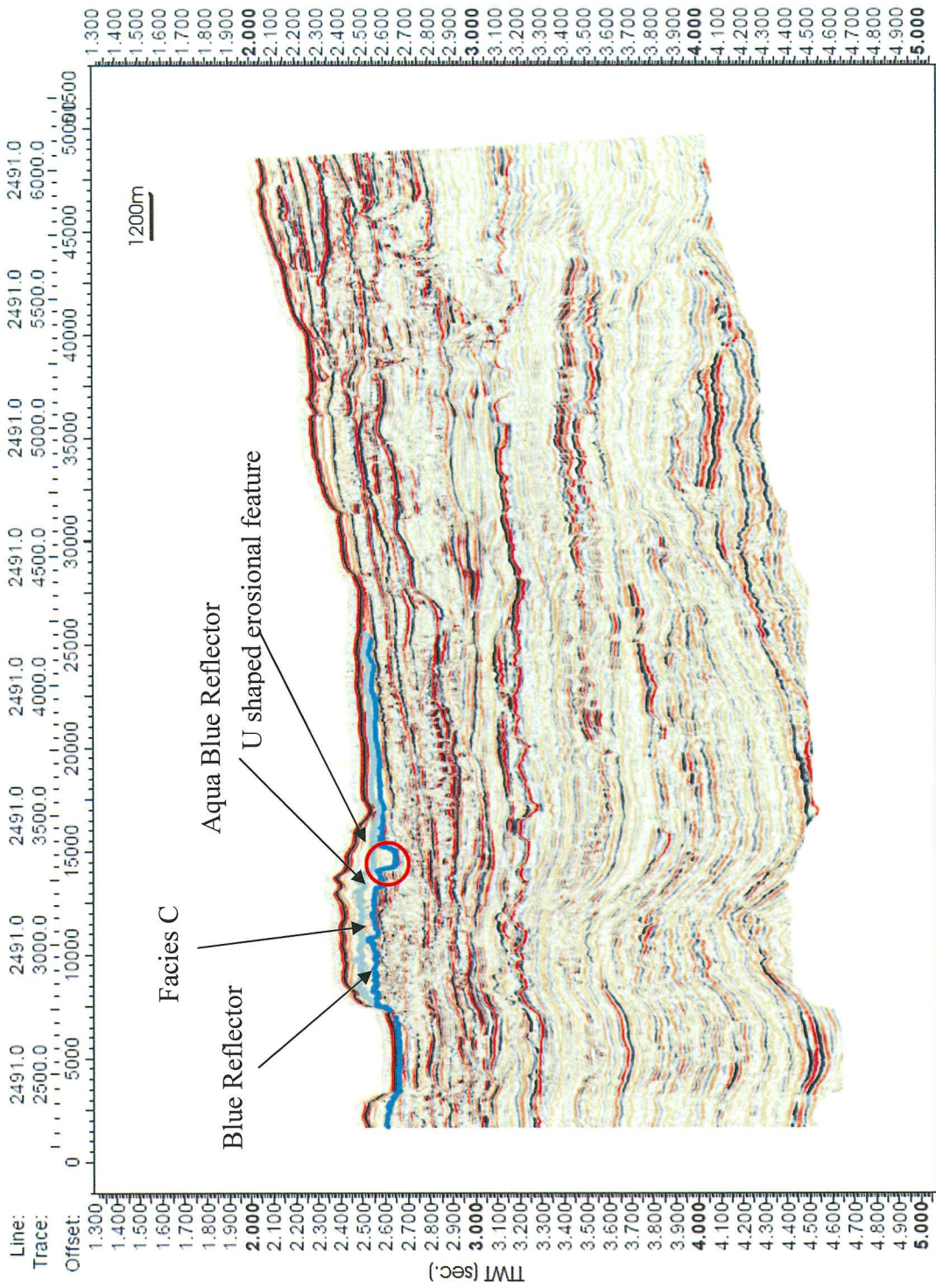
Figure 4.9 – Blue-Aqua Blue unit seen in Strike line 2491

34

4.4 Errors and Data Limitations

There are limits to resolution of the data within the Barrington cube, software error and human error has to be considered based on the ability that reflectors could be picked as a result of the incoherence of the data. Software error can include bad auto-picking or display artefacts'. When the horizons are rendered in the 3D mode of Kingdom Suite, there are sometimes holes within the data surfaces. Some of these surfaces have been re-picked at closer intervals and then rendered again. Holes remained in the newly rendered surface indicating the incoherence of the data in some areas.

4.4.1 Temporal (Vertical) Resolution

Temporal resolution for 3D seismics is estimated by the Rayleigh criteria through the use of ¼λ of a seismic signal where λ is the wavelength. To define the smallest resolvable target the maximum frequency needs to be known. If a spectrum of frequencies is used, then a range of targets can be resolved. This will provide the best resolution and is known as a temporal bandwidth. This bandwidth is dependant on the source spectrum (including the ghost effect and instrument response), absorption function, receiver depth, single element spacing and the temporal noise spectrum. The shot receiver that is closest to the output will be the determining factor for the vertical resolution. The best vertical resolution is obtained in the near offset traces because the angle of incidence is nearly vertical. The water depth is another factor when dealing with vertical resolution. As the water depth increases the angle of incidence decreases with the same shot-receiver spread (Mosher *et al.*, 2006).

4.4.2 Spatial (Horizontal) Resolution

Spatial resolution for un-migrated 3D seismics depends mainly on the dimension of the Fresnel Zone. When "energy is returned to a detector within a half a wavelength of the initial wavelength of the initial reflected arrival interferes constructively to build up the reflected signal" (Kearey *et al.*, 2002). The Fresnel Zone is the part of the interface in which this energy has been returned (Kearey *et al.*, 2002). Figure 4.10 illustrates the Fresnel Zone.

Source

λ/4

Reflector
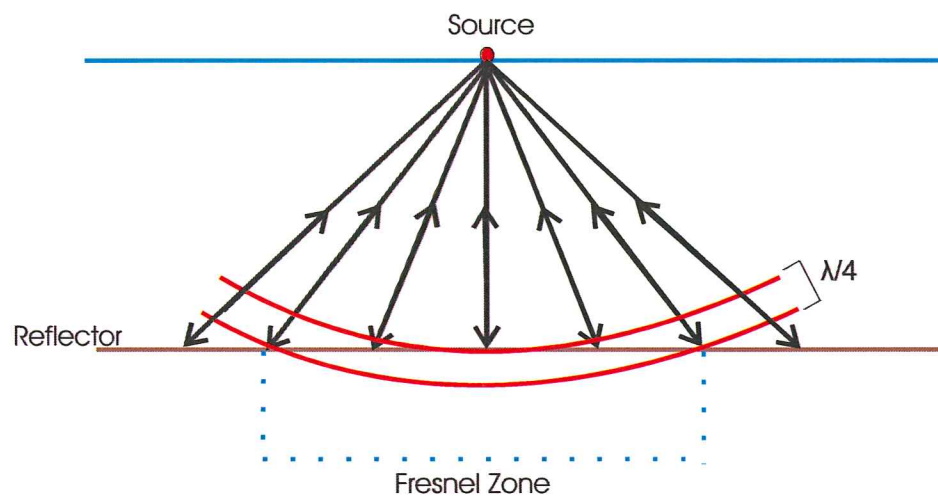
Fresnel Zone

Figure 4.10 – The part of the reflector that returns energy within half a wavelength from the initial reflected arrival is known as the Fresnel Zone. (Modified from Kearey *et al.*, 2002).

When acoustic energy is emitted, the ray paths expand radially, so when imaging the acoustic pulse it is actually a zone that is formed rather then a point on a bedding interface that is being imaged. The dominant wavelength of the source wavelet determines the Fresnel Zone and is the region where the constructive interference surrounding the geometrically predicted reflection point (Mosher *et al.*, 2006). To illustrate this, we can look at how the Fresnel Zone behaves in response to varying

sandstone bodies. As a sandstone body reaches or becomes smaller than the lateral

dimension of a Fresnel Zone, the reflection character of the reflector is diminished. So

thin sandstone beds with spatial extent will have a seismic expression, but without a

strong reflective nature. As well, sandstones that are smaller then the Fresnel Zone will

have similar signatures but their sizes can be gauged based on the strength of the seismic

reflections. These trends can be seen in Figure 4.11 (from Neidell and Poggiagliolmi,

1977). When migrating 3D seismic data as has been done with Barrington data, the

Fresnel zone will collapse in two directions. As a result of data migration, the Fresnel

zone is not a factor for spatial resolution. When considering spatial resolution the

acoustic aperture, the pattern responses and group interval, the hydrophone spacing and

the spatial noise power spectrum also have to be considered and included. Two

important factors are the frequency and acoustic aperture and they are summarized in the

figure 4.11.
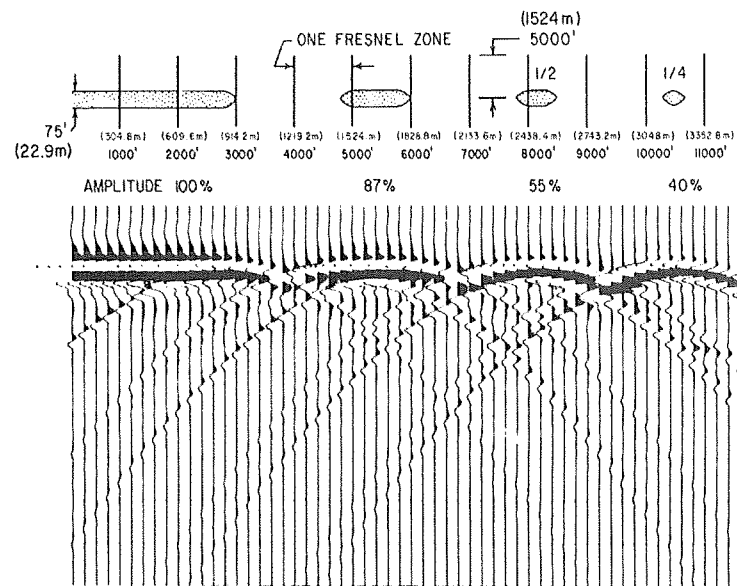
Figure 4.11 – The seismic section displays the seismic signature of sandstone bodies with varies lateral extents and the significance of the Fresnel Zone size. The smaller sand bodies produce weaker reflections because they occupy smaller portions of the Fresnel Zone (from Neidell and Poggiagliolmi, 1977).

37
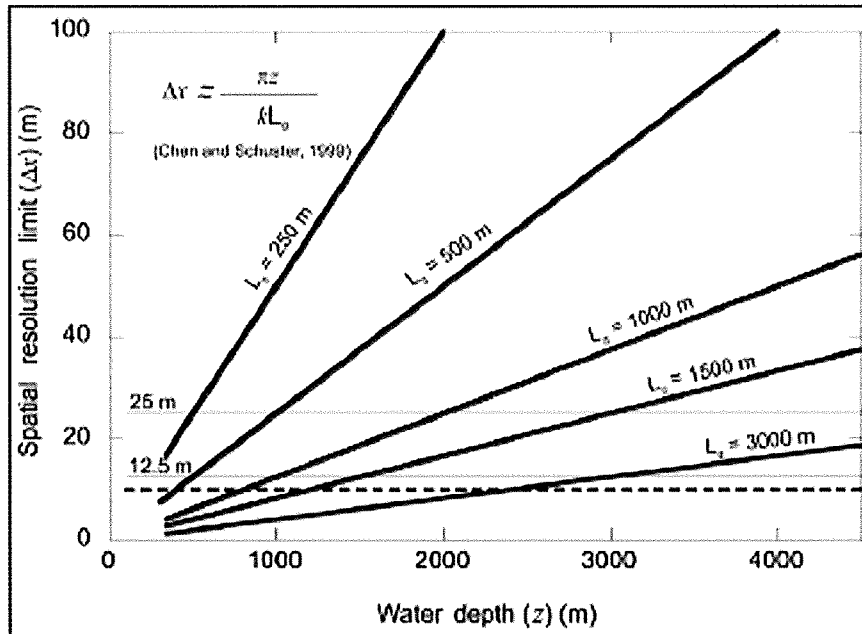
Figure 4.12 – This graph shows that for larger apertures, the spatial resolution is dependent on bin size. With shorter source-receiver offsets or greater water depths the resolution is controlled by the length of the acoustic aperture. With shallower water depths the cross line aperture will be the largest spatial resolution restriction (Mosher *et al.*, 2006).

Figure 4.12 shows that wider apertures and wider bandwidths increase lateral resolution (Mosher *et al.*, 2006). Cross-line spatial resolution will be less then in-line spatial resolution because of the shorter aperture length. Along with the acoustic aperture, the receiver channel spacing and the number of receiver channels may also need to be considered. The farthest shot receiver pair will provide the best spatial resolution (Mosher *et al.*, 2006).

When processing the data after migration, typically the seafloor and near-seafloor returns are muted to prevent stacking of far off-set traces when the NMO is stretched

38

reducing the frequency of the trace. This process can affect the spatial resolution (Mosher *et al.*, 2006).

Bin dimensions, stacking fold and errors associated with common mid-point also have to be considered for spatial resolution in 3D seismic data. For most surveys, the bin dimensions are larger than the acoustic resolution causing the bin dimension to be the factor for resolvability of a target. The inline sub-surface bin is 12.5m while the crossline was 37.5 m. In order to resolve a target two to three samples are required and for 12.5 grid spacing, which the Barrington Cube is, the resolvability of a target must be at least 25 to 50 m. Cross-line trace spacing is smaller than the in-line trace spacing making the resolution in the in-line direction greater (Mosher *et al.*, 2006).

Chapter 5: Discussion and Conclusions

5.1 Introduction

This chapter will interpret the genesis of the six seismic units described in Chapter 4 as well as their possible triggering mechanisms.

5.2 Interpretation of Seismic Units

5.2.1 Red-Royal Blue Unit

The Red horizon that forms the base of the Red-Royal Blue unit is interpreted as a large scale erosional surface across the study area. Evidence to support this interpretation includes truncation of underlying reflectors (Fig. 5.1) and presence of channels (Fig. 5.1). The Red-Royal Blue unit is dominated by Facies A (refer to Fig 4.1) with some of the wavy reflections terminating into other reflectors. Within this unit there is one erosional sediment filled channel (Fig 5.2). This unit is interpreted as a turbidite flow based on the high amplitude, parallel reflectors.

Red Horizon Truncation
Black Reflector

1200 m

Sediment Filled
Channels
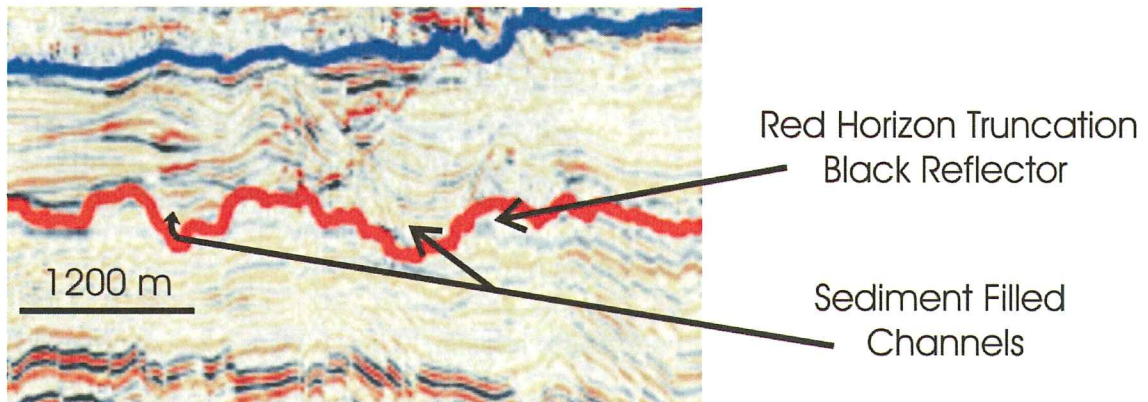
Figure 5.1 – Truncated reflectors and channels as evidence for an erosional surface (large scale unconformity).

Sediment filled channel

1200 m
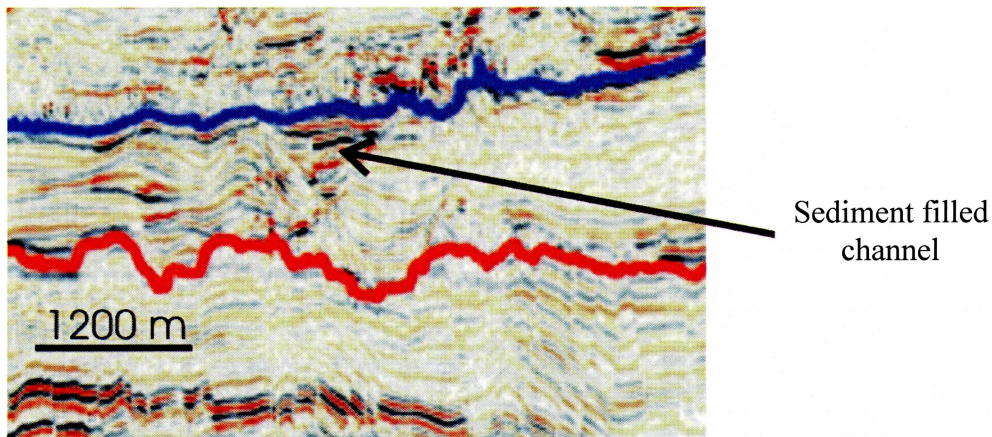
Figure 5.2 – Channel in the Red-Royal Blue Unit.

5.2.2 Royal Blue-Orange unit

The Royal Blue horizon is the base of the Royal Blue-Orange unit and is the top of the Red-Royal Blue unit. This horizon is an erosional surface that is correlated across the study area. Truncation by this erosional surface isn't as easily seen as in the Red-Royal Blue unit but is shown in Figure 5.3. The Royal Blue-Orange unit is

Blue horizon truncating underlying reflectors

1200 m
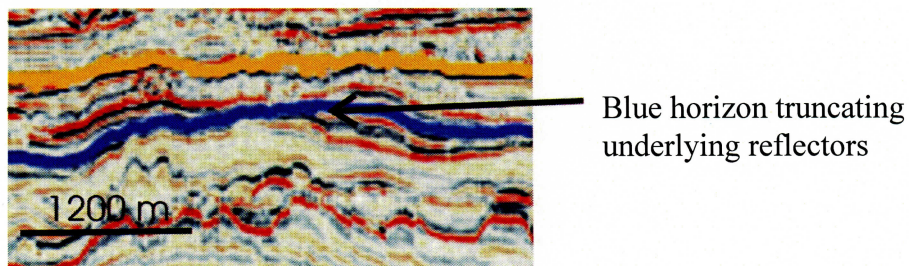
Figure 5.3 – Truncated Reflectors

characterized by Facies B and C (chaotic reflectors) (refer to Fig 4.1). The areas that contain Facies A have reflectors that converge and diverge. The low and high amplitude chaotic reflectors seen in this unit are typically deposited in topographic lows on the slope or basin floor. The occurrence of contorted and discordant to wavy sub-parallel reflections, hummocky reflections at the top of the unit (Fig 5.4), and erosional gouges

(Fig 5.4) into the Red-Royal Blue unit are used as evidence to interpret this unit as a mass transport complex.
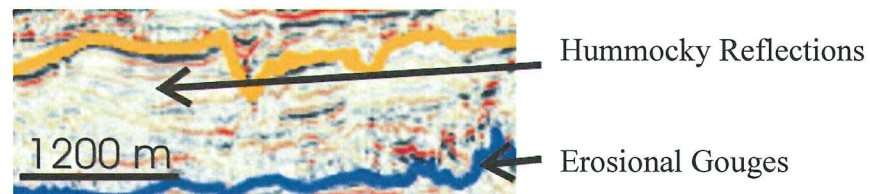
Figure 5.4 – Examples of hummocky reflections and erosional gouges.

5.2.3 Orange-Green unit

The Orange horizon is interpreted as an erosional surface that contains several channels and truncates reflectors from the Royal Blue-Orange unit. This surface is easily correlated across the study area. The occurrence of hummocky reflectors in the top of the unit, an erosional base (Fig 5.5) as well as the chaotic nature of the Orange-Green unit as described by Facies B (chaotic reflectors) are use elements used to interpret this unit is mass transport complex.
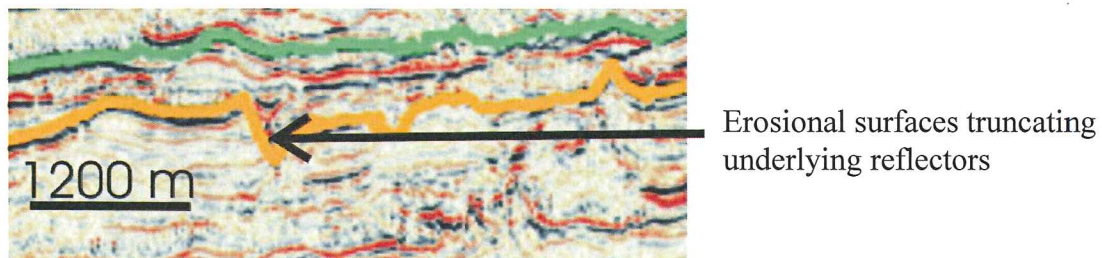
Figure 5.5 – Erosional base for the Orange-Green unit.

5.2.4 Green-Yellow unit

The Green horizon is interpreted as an erosional surface that truncates reflectors from the Orange-Green unit. The Green horizon is easily correlated across the study

area. This unit is characterized by Facies B (chaotic reflectors) with the presence of hummocky reflectors at the top of the unit, an erosional base and the chaotic nature of the reflectors provide evidence that this unit is a mass transport complex.

5.2.5 Blue-Aqua Blue unit

The Blue-Aqua Blue unit is found within the Yellow-Yellow (seafloor) unit (refer to Table 4.1). The Blue horizon is the base of this unit and is an erosional surface that truncates the Yellow horizon. Correlation of the Blue horizon and the Aqua Blue horizon can not be done across the study area, making it a localized feature. This unit has an erosional base, but due to the relatively thin nature of the unit, the hummocky reflectors can not be seen. Based on the erosional base and presence of Facies C (chaotic reflectors), this unit is interpreted as a mass transport complex deposit.

5.2.6 Yellow-Seafloor unit

The Yellow horizon is the base of this unit which can be correlated across the study area except for where the Blue horizon truncates it. The top bounding horizon for this unit is the Seafloor Horizon which can be easily correlated across the study area. The Yellow-Seafloor unit is dominated by Facies D with the north-eastern end being dominated by Facies A. The reflectors within this unit are mostly parallel with low amplitudes. This unit has been interpreted as Holocene sediments.

5.2.7 MTC Order

Beginning at the base of the focused seismic data for this project we have a large unconformity (Red horizon) that is easily correlated across study area followed by a package of sub-parallel to parallel reflectors topped with study wide erosion surface (Royal Blue horizon). There are four MTC's stacked on top of each other (Fig 5.6),

above this sub-parallel to parallel package with the three lower MTC's having their bounding horizons easily correlated across the area. The fourth MTC (Blue-Aqua Blue unit) is a localized event in this study area but is found on three large scale MTC events. The upper most unit of the Barrington Cube is another package of sub-parallel to parallel reflectors with the seafloor pick being the top horizon picked.
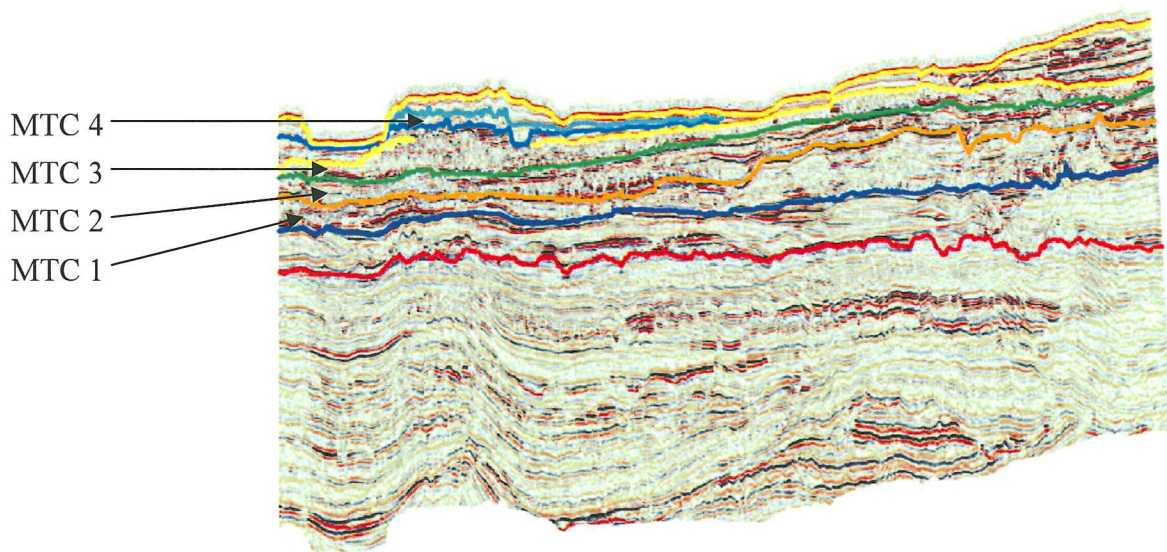
Figure 5.6 - The four mass transport complexes stacked on top of each other.

5.3 Stratigraphic Framework - Interpretation of Mass Transport Complexes

Mass transport complex deposits (MTC) are one of the key components which contribute to the present Scotian Slope. It is key to be able to map these MTC's over large areas in order to understand the stratigraphic relationships between the various events that are of focus for this thesis project. Mass transport complexes have been defined by Weimer (1990) as "sediments that occur at the base of sequences and are overlain and/or onlapped by channel and levee sediments. They commonly overlie an

erosional base up-slope and become mounded down-slope, are externally mounded in shape, and pinch out laterally." The term mass transport complexes was initially coined when referring to seismic stratigraphy but is becoming a more common phrase to describe mass failures in general. Mass transport complexes can be described as chaotic deposits which contain deformed rafts of disrupted bedding of conglomerates, mudstones, breccias and sandstones. MTC's is a term used to describe a large range of deposits and is typically used since it is less process-specific (Pickering and Corregidor, 2005). MTC deposits are common in the Barrington cube and are the most important features in the construction of the margin in this area.

Identifying seismic units based on seismic facies is one method of a descriptive classification, but does not necessary provide an interpretation of a specific depositional environment as an individual seismic facies can be produced by more than one depositional process. A mass transport complex deposit can be constructed of one or several mass failures with episodes of construction and erosion. MTC's can have a variety of characteristics in terms of shape, size, area, geomorphology and seismic character, all of which may vary as it is deposited down slope of the point of origin. Truncations and incoherency of reflectors are some of the indicators used to determine if seismic units are mass transport complexes. MTC's characteristic chaotic reflections, as seen in seismic profiles, can be explained by disruption of bedding structure and stratigraphy during the failure process. Due to the large distances which MTC's can travel, not all features used to classify a MTC or the components that constructed the MTC will be necessarily present. In all deposits, occurrences of hummocky reflections

with chaotic or incoherent reflectors, as well as an erosional base are key seismic indicators used to identify a MTC (Table 5.1).

Criteria Used to Identify MTC's
Truncation of Reflectors
Incoherency of Reflectors
Chaotic Reflectors
Hummocky Reflectors
Erosional Base

Table 5.1 – Criteria used through this thesis to interpret the Seismic Units as Mass Transport Complex Deposit (Modified from Sangree and Widmier, 1979).

5.4 Possible Trigger Mechanisms

The Scotian margin offshore Nova Scotia has been, and continues to be, influenced by geological events and processes including seismicity, glaciation, gas hydrates and salt tectonics. Some of these events have had a larger impact on the events recorded along the Scotian margin then others but to associate one trigger mechanism to a specific event can be very difficult.

5.4.1 Seismicity

Seismicity has been the trigger mechanism for many MTC's. It is sometimes hard to record their effects as they may occur in clusters. The Scotian margin shows that smaller events are more frequent and more likely to happen but large seismic events have occurred in the past that have proved to be significant in Atlantic Canada.

The only MTC for which we know the trigger mechanism is the 1929 event which was triggered by a M7.2 earthquake, with its epicentre located at 44°30' N and 57°15' W. The depth of the earthquake was estimated at 20 km beneath the seafloor of the Grand Banks off the mouth of the Laurentian Channel in the North Atlantic. The earthquake itself caused no damage but the resulting landslide triggered a tsunami that killed 28 people and destroyed the communities in the Burin Inlet. The turbidity current was a result of the slump that formed on the continental slope which carried sediment up to 1000 km southward on the Atlantic seafloor (Fine *et al.*, 2005) and broke 12 trans-Atlantic telegraph cables up to 500 km from the epicentre. The turbidity flow had an estimated thickness of several hundred meters and duration of up to eleven hours (Piper *et al.*, 1988).

5.4.2 Glaciation

The Scotian Slope has been influenced by past glaciations from the mid-Pleistocene to the Late Wisconsinian as described by King and Fader (1986), Piper and Normak (1989) and Mosher *et al.* (2004) and others. During these times large amounts of sediments were deposited along the slope causing it to become unstable. This scenario has been documented on other continental margins such as the Antarctic margin and the Norwegian continental slope. The Gebra Slide occurred on the Trinity Peninsula, Central Bransfield Basin, Antarctic Peninsula. It was a smaller scale event than those that occurred in the North Atlantic, but it also underwent high rates of sedimentation during the last glaciation along with unloading of the retreating ice sheet. These deposits along with the retreating ice sheet may have created higher then normal pore pressures leading the deposits to be fluidized and subject to failure (Imbo *et al.*, 2003).

The instability created by the sediment overloading during glacial periods have been suggested as triggering mechanisms for mass transports along other margins and is likely a factor on the Scotian margin.

5.4.3 Gas Hydrates

The Storegga Slide which occurred off the Norwegian continental margin has been suggested to be related to gas and gas hydrates (Bugge et al., 1988). The occurrence of a bottom simulating reflector (BSR) in seismic profiles provides evidence for the presence of gas hydrates. As gas hydrates decompose from a solid to a liquid, the free gas increases the pore fluid pressure weakening the strength of the sediments. This weakening of sediments is associated with sediment mobilisation and a possible trigger mechanism for the slide (Posewang and Mienert, 1999).

Gas hydrates can change with glacial and interglacial periods as result of pressure and temperature changes. Mosher et al. (2004) discuss the possibility of gas hydrates being a factor in the mass transport complexes found offshore Nova Scotia.

BSR's have been located on the Scotian margin (Mosher et al., 2004) indicating the presence of gas hydrates on the Scotian Slope. Their occurrence has to be considered when trying to determine a trigger mechanism for the mass transport complexes that have occurred in the sediment record on the Scotian Slope.

5.4.4 Salt Tectonics

In the Gulf of Mexico, during interglacial and glacial times halokinetic processes occurred. In the interglacial time the salt adjustment occurred as a result of erosional and depositional environments where in the last glacial period, significant sedimentation occurred causing the re-adjustments. The re-adjustments that took place during the

glacial period probably were the triggering mechanisms for the most observed sediment failures in this area. The over steepening of basin flanks as a result of salt diapirism can be significant reason for slope instabilities in this region (Lee *et al.*, 1996).

The re-adjustment and over steepening of basin flanks caused by salt diapirism as discussed by Lee *et al.* (1996) can be seen in areas of the Barrington Cube. The slope instability created by this over steepening can be easily be considered as one of the triggering mechanisms for the MTC's that are seen within the project area.

5.5 Conclusions

The Barrington cube provides good examples of some of the processes modifying the past and present Scotian Slope, in terms of mass transport complexes. There are four MTC's stacked on top of each within the data and they are correlatable across the study area suggesting that these events were episodic widespread failures.

The triggering mechanisms for these MTC's include seismic events, glacial sediment overloading, gas hydrates and salt tectonics. All the mass transport complexes seen within the Barrington Cube occur on the Slope indicating that gravitational forces play an important role in these features (Mosher *et al.*, 1994). The only sediment failure event for which the trigger mechanism is known is the 1929 Grand Banks Earthquake. Most triggering events are a combination of the four mechanisms, with glacial periods possibly influencing each event. It has been suggested that during glacial periods, that seismicity induced by glacial loading and unloading can be accounted for the shallower slope failures. The adjustment of salt diapirs as a result of glacial sediment loading can over steepen basin flanks causing the slope to become unstable leading to failures. When sea levels fell during glacial periods, the decrease in pressure and temperature could have

destabilized gas hydrates inducing slope failures as suggested by Piper and Campbell (submitted). Gas hydrate dissociation resulting in excess pore pressure caused by the loading of till tongues during glacial deposition could also have lead to slope failure (Gauley, 2001). The increase of bottom water temperatures on the southwestern Scotian margin as a result of Gulf Stream rings during interglacial times could have also lead to gas hydrate dissociation (Piper *et al.*, 2003). The combination of mechanism discussed could have resulted in the triggering of the MTC's seen in this project but do to their size, it has been suggested that a regional event is required to initiate this scale of failure. The scale of the mass failures found within the Barrington cube are only located along certain portions of the Scotian margin, further supporting that the triggering mechanisms must be of a regional scale. The only regional events occurring along the Scotian margin that could likely trigger these events would be the passive margin earthquakes. With the occurrence of three M>7 earthquakes since 1800 on Canada's eastern margin, the resulting seismicity could initiated an event like the 1929 Grand Banks Earthquake (Piper and McCall, 2003). It must be kept in mind though that most trigger mechanisms for mass sediment failures are unknown or poorly understood.

The Cenozoic stratigraphy of the Scotian Slope that has been developed during this project increases the understanding of how mass transport complexes have influenced the evolution of the Scotian margin. By interrupting the deposits found in the Barrington Block as MTC's, a better understanding of how sediment transport to deep water basins occurs and how it affects their development. Although we cannot identify the particular trigger mechanisms for each of these events, the occurrence of passive

margin earthquakes with large magnitudes and gas hydrate dissociation has to be kept in mind when completing geo-hazard assessments for potential Industry activity.

5.6 Future Work

The Barrington Cube is a large data set which could be re-picked focusing on smaller scale events or deeper events then what this project looked at. New attributes are being created for seismic interpretation which highlights features in a new way, possibly providing new interpretation and ideas on older conclusions. Within the Barrington block, grounding-truthing through deep and shallow cores would allow sediment analysis and possible age dating of shallower MTCs. With future work building on the accomplishments of this project, the development of models for deep water basin off the Scotian margin will assist in future geo-hazard assessments required for potential offshore exploration and development.

References

Adams, J. and Halchuk, S. 2003. Fourth generation seismic hazard maps of Canada: Values for over 650 Canadian localities intended for the 2005 National Building Code of Canada, Geological Survey of Canada Open File 4459.

Campbell, D.C., Shimeld, J.W., Mosher, D.C., Piper, D.J.W. 2004. Relationships Between sediment mass-failure modes and magnitudes in the evolution of the Scotian Slope, offshore Nova Scotia. Offshore Technology Conference. OTC 16743. Houston.

Bugge, T., Belderson, R.H. and Kenyon, N.H. 1988. The Storegga Slide. Philosophical Transactions of the Royal Society of London. Series A, Mathematical and Physical Sciences, V. 325, No. 1586, p. 357-388.

Emery, K.O., Uchupi, E. 1984. The Geology of the Atlantic Ocean. Springer-Verlag. New York.

Figure 2.1. Retrieved from http://gsc.nrcan.gc.ca/marine/scotianmargin/so_e.php on the World Wide Web on November 2, 2006. Web page last updated on 2006-02-03.

Figure 3.1. Retrieved from www.acsonline.org/issues/sound/images/seismicShip Config.jpg on the World Wide Web, February 26, 2007.

Fine, I.V., Rabinovich, A.B., Bornhold, B.D., Thomson, R.E. and Kulikov, E.A. 2005. The Grand Banks landslide-generated tsunami of November 18, 1929: Preliminary analysis and numerical modeling. Marine Geology 215, 45-57.

Gauley, B.J.L. 2001. Lithostratigraphy and sediment failure on the central Scotian Slope. M.Sc. Thesis. Dalhousie University, Halifax, Nova Scotia, Canada.

Gemmer, L., Ings, S., Medvedev, S., Beaumont, C. 2004. Salt tectonics driven by differential sediment loading: stability analysis and finite-element experiments. Basin Research 16, 199-218.

Hart, B. 2000. 3-D Seismic Interpretation: A Primer for Geologists. SEPM Short Course No. 48.

Imbo, Y., De Batist, M., Canals, M., Prieto, M.J., and Baraza, J. 2003. The Gebra Slide: A submarine slide on the Trinity Peninsula Margin, Antarctica. Marine Geology 193, 235-252.

Mosher, D.C., Bigg, S., LaPierre, A. 2006. 3D seismic versus multibeam sonar seafloor Surface renderings for geohazard assessment: Case examples from the central Scotian Slope. The Leading Edge, December 2006, 1484-1494.

Neidell, N.S. and Poggiagliolmi, E. 1977. Stratigraphic Modelling and Interpreation – Geophysical Principles and Techniques. Seismic Stratigraphy – applications to Hydrocarbon exploration, Memoir 26, edited by Payton, C.E. The American Association of Petroleum Geologists, Tulsa, Oklahoma, USA.

Pickering, K.T. and Corregidor, J. 2005. Mass-Transport Complexes (MTCs) and Tectonic Control on Basin-Floor Submarine Fans, Middle Eocene, South Spanish Pyrenees. Journal of Sedimentary Research, V. 75, 761-783.

Piper, D.J.W. and Campbell, D.C. Submitted. Quaternary geology of Flemish Pass and its application to geohazard evaluation for hydrocarbon development. In Petroleum Resources and Reservoirs of the Grand Banks, eastern Canada margin, ed. R.N. Hiscott and A. Pulham. Geological Assoication of Canada Special Publication.

Piper, D.J.W. Late Cenozoic geological framework of the Scotian Slope and its impact on hazards that affect offshore hydrocarbon exploration and development. Geological Survey of Canada (Atlantic), Bedford Institute of Oceanogarphy.

Piper, D.J.W., Farre, J.A., and Shor, A.N. 1985. Late Quaternary slumps and debris Flows on the Scotian Slope. Geological Society of America Bulletin, 96: 1508-1571.

Piper, D.J.W., Shor, A.N., Hughes Clarke, J.E. 1988. The 1929 "Grand Banks" Earthquake, Slump and Turbidity Current (Clifton, H.E., Ed.). Special Paper – Geological Society of America, 229, 77-92.

Piper, D.J.W. and Normak, W.R. 1989. Late Cenozoic sea level changes and the onset of glaciation: Impact on continental slope progradation off eastern Canada: Marine and Petroleum Geology. V. 6, p. 336-348.

Piper DJW and Sparkes R (1990) Pliocene-Quaternary geology, Central Scotian Slope. Geological Survey of Canada Open File 2233, 2 p + 12 maps.

Piper, D.J.W. and Skene, K.L. 1998. Latest Pleistocene ice-rafting events on the Scotian Margin (eastern Canada) and their relationship to Heinrich events. Paleoceanography 13, 205-214.

Piper, D.J.C. and McCall, C. 2003. A synthesis of the Distribution of submarine mass Movements on the eastern Canadian margin. Geological Survey of Canada (Atlantic), Bedford Institute of Oceanogarphy.

Piper, D.J.W., Mosher, D.C., Gauley, B.-J., Jenner, K. and Campbell, D.C. 2003. The Chronology and recurrence of submarine mass movements on the continental Slope off southeastern Canada. Geological Survey of Canada (Atlantic), Bedford Institute of Oceanogarphy.

Posewang, J. and Mienert, J. 1999. The enigma of double BSRs: indicators for changes in the hydrate stability field?. Geo-Marine Letters 19, p 157-163.

Retrieved from the World Wide Web site NRCAN on January 14, 2007 from http://earthquakescanada. nrcan.gc.ca/zones/eastcan_e.php#LSSZ. This webpage was last updated on February 23, 2006.

Sangree, J.B, and Widmier, J.M. 1979. Interpretation of depositional facies from seismic data. Geophysics, V., 44, p. 131-160.

Shimeld, J., Jackson A., Wade, J., Dehler, S., Piper, D., Funck, T., Post, P., Olson, D. 2004. A Comparison of Salt Tectonic Subprovinces Beneath the Scotian Slope and Laurentian Fan. GSC Contribution N0. 2004025.

Shaw, J. and Courtney, R.C. 2002. Postglacial Coastlines of Atlantic Canada: Digital Images. Open File 4302. Geological Survey of Canada, Ottawa.

Thurman, H.V., Trujillo, A.P. 2002. Essentials of Oceanography 7th Edition. Prentice Hall. New Jersey.

Wade, J. and MacLean, B. 1990. The geology of the southern margin of Canada. In Geology of the continental margin of eastern Canada. Edited by M.J.Keen and G.L. Williams. Geological Survey of Canada Geology of Canada No. 2, Chap 5.

Weimer, P. 1990. Sequence Stratigraphy, facies geometries, and depositional history of the Mississippi Fan, Gulf of Mexico. American Association of Petroleum Geologists Bulletin (0149-1423), V. 74, Iss 4, p. 425-453.